INVESTIGATION OF THE POSSIBILITIES FOR ELECTRO-CHEMICAL CONTROL OF HOT CORROSION MECHANISMS

ARTHUR D. LITTLE, INCORPORATED

PREPARED FOR

NAVAL AIR DEVELOPMENT CENTER

APRIL 1974

AD 787055

SECURITY CLASSIFICATION OF THIS PAGE (When Data Entered)

REPORT DOCUMENTATION PAGE

READ INSTRUCTIONS BEFORE COMPLETING FORM

1. REPORT NUMBER
2. GOVT ACCESSION NO.
3. RECIPIENT'S CATALOG NUMBER

4. TITLE (and Subtitle)
INVESTIGATION OF THE POSSIBILITIES FOR ELECTRO-CHEMICAL CONTROL OF HOT CORROSION MECHANISMS

5. TYPE OF REPORT & PERIOD COVERED
FINAL REPORT
December 1972 to Dec. 1973

6. PERFORMING ORG. REPORT NUMBER
75526

7. AUTHOR(s)
Dr. Joan B. Berkowitz
W. David Lee

8. CONTRACT OR GRANT NUMBER(s)
Contract No. N62269-73-C-0288

9. PERFORMING ORGANIZATION NAME AND ADDRESS
ARTHUR D. LITTLE, INC.
20 Acorn Park
Cambridge, Mass. 02140

10. PROGRAM ELEMENT, PROJECT, TASK AREA & WORK UNIT NUMBERS

11. CONTROLLING OFFICE NAME AND ADDRESS
Naval Air Systems Command
Department of the Navy
Washington, D.C. 20361

12. REPORT DATE
APRIL 1974

13. NUMBER OF PAGES
60

14. MONITORING AGENCY NAME & ADDRESS(if different from Controlling Office)
Naval Air Development Center
Warminster, Pennsylvania 18974

15. SECURITY CLASS. (of this report)
UNCLASSIFIED

15a. DECLASSIFICATION/DOWNGRADING SCHEDULE

16. DISTRIBUTION STATEMENT (of this Report)
"APPROVAL FOR PUBLIC RELEASE DISTRIBUTION UNLIMITED"

17. DISTRIBUTION STATEMENT (of the abstract entered in Block 20, if different from Report)

18. SUPPLEMENTARY NOTES

19. KEY WORDS (Continue on reverse side if necessary and identify by block number)
Hot corrosion
Molten sodium sulfate
Sodium sulfate seeded flames
Flame conductivity
Nichrome
Inconel 600
Wagner mechanism

20. ABSTRACT (Continue on reverse side if necessary and identify by block number)
The effect of applied currents on the hot corrosion of nickel, pure Nichrome, Inconel 600, Hastellow X, and a Co-Cr-Al-Y alloy in both sodium sulfate melts and a sodium sulfate seeded flame has been briefly investigated. In the molten salt bath, some evidence of anodic protection was observed with strip samples of the chromia forming alloys, Nichrome and Inconel 600. Polished spherical samples of Inconel 600 were not corroded by the molten salt until structural defects were introduced either by abrading the surface or by

DD FORM 1 JAN 73 1473 EDITION OF 1 NOV 65 IS OBSOLETE
S/N 0102-014-6601

SECURITY CLASSIFICATION OF THIS PAGE (When Data Entered)

application of high anodic or cathodic currents. In the salt seeded flame, the rate of corrosion was affected very little by applied currents, probably because of the low current densities achievable in a flame system. Evidence was obtained for a difference in mechanism between anodically and cathodically polarized Nichrome samples, oxidation being more pronounced at the cathode and sulfidation at the anode. In addition, alkali metal tends to penetrate deeply into the cathodic samples, while remaining on the surface of the anodic samples.

"APPROVED FOR PUBLIC RELEASE
DISTRIBUTION UNLIMITED"

FINAL REPORT

INVESTIGATION OF THE POSSIBILITIES FOR ELECTROCHEMICAL CONTROL OF HOT CORROSION MECHANISMS

Authors:

Joan B. Berkowitz
W. David Lee

Prepared Under Contract No. N62269-73-C-0288
Naval Air Development Center
Warminster, Pennsylvania 18974

for

Naval Air Systems Command
Department of the Navy
Washington, D.C. 20361
Attention: I. Machlin
AIR 52031B

ib

TABLE OF CONTENTS

I. INTRODUCTION

A. INFLUENCE OF ELECTRIC FIELDS ON SCALE GROWTH KINETICS

The electrochemical nature of oxidation and hot corrosion reactions has been recognized for a long time. The Wagner theory of high temperature parabolic oxidation, for example, is frequently discussed in terms of an electrochemical cell analogue in which the growing oxide film serves both as the cell electrolyte for ionic transport, and as the external circuit for conduction of electrons.

In the interaction of gases with pure metals it is known that parabolic growth of an ionically conducting solid reaction product, via a true Wagner mechanism, can be inhibited and even stopped by application of an electric field across the growing layer of reaction product. The effect has been demonstrated experimentally for the oxidation of zinc[1] and silicon.[2] In both cases, in agreement with theory, oxidation was retarded when the metal/metal oxide interface was negative with respect to the oxide/gas interface and accelerated when the polarities were reversed. That is, the retarding field is applied so that the flux of oxygen ions inward and metal ions outward is decreased, while the accelerating field enhances the ionic transport associated with parabolic oxidation.

Wagner has pointed out[3] that it is impossible to modify the electric field in a growing oxide phase without passing a net electrical current. As indicated in Figure 1, the effect of an electrical current's flowing across an oxide layer may be described as a solid state electrolysis. When the air/oxide interface is negative with respect to the oxide/metal interface, the net reaction is the formation of the oxide or an enhancement of oxidation rate. When the air/oxide interface is positive with respect to the oxide/metal interface, electrolysis results in a decomposition of the oxide or a decrease in over-all oxidation rate. The quantitative theory has been discussed by Kröger,[4][5] Wagner, and Kofstad.[6] Following Kofstad, we find that if a metal, M, corrodes with the formation of a single phase oxide scale, M_aO_b, then the passage of a current, I_{ext}, through the scale will result in a growth rate, dn/dt, which differs from the growth rate under zero current conditions, $\left(\frac{dn}{dt}\right)_o$, as follows:

$$\frac{dn}{dt} = \left(\frac{dn}{dt}\right)_o - \frac{I_{ext}}{erb}\ (t_M + t_X) \qquad (1)$$

where n, in molecules/cm^2, is the number of molecules of scale accumulated on each square centimeter of metal surface at time t; e is the electronic charge; r is the valence of the negative ions; t_M and t_X are transference numbers of the positive and negative ions respectively. In terms of electronic potential, E_{ext}, across the growing scale of thickness Δx, the growth rate is expressed by:

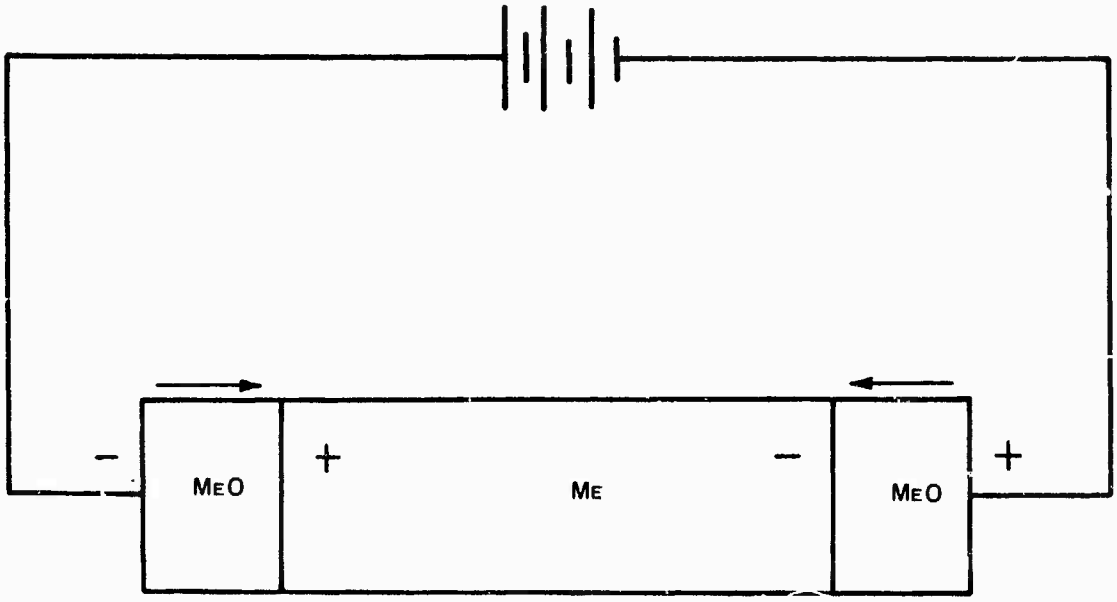

$$ME/MEO:\ ME \longrightarrow ME^{++} + 2e^{-}$$

$$\underline{OR}\ O^{=} + ME \rightleftharpoons MEO + 2e^{-}$$

$$O_2/MEO:\ ME^{++} + \frac{1}{2}O_2 + 2e^{=} \rightleftharpoons MEO$$

$$\underline{OR}\ \frac{1}{2}O_2 + 2e^{=} \rightleftharpoons O^{=}$$

$$NET:\ ME + \frac{1}{2}O_2 \rightleftharpoons MEO$$

FIGURE 1

Electrochemical Interface Reaction When
An Electric Field is Improved Across a Growing
Oxide Film

$$\frac{dn}{dt} = \frac{(t_M + t_X)(\sigma)(E-E_{ext})}{erb\ \Delta x} \qquad (2)$$

where σ is the conductivity of the scale and E is the voltage change associated with the free energy ΔG of the corrosion reaction (ΔG=EbrF, where F is the Faraday constant). A retarding potential of magnitude $E_{ext} = E$ should completely stop oxidation or scaling.

The observed effects of electric fields on parabolic oxidation, when the controlling factor is diffusion of metal or oxygen species through a growing scale, is clearly dependent on the ionic nature of the diffusing species. In order for corrosion rates to be significantly different in the presence and absence of imposed electric fields, it is necessary for the ionic transport to be significant compared to the electronic. Thus, if the scale is a pure electronic conductor, ($t_e = 1$ and t_M [illegible] $= 0$), electric fields should not influence the corrosion rate, provided that Equation (2) is valid for the system under investigation. Naturally, if oxidation or scaling is controlled by diffusion of neutral atomic or molecular species, no significant field effects are to be anticipated. On the other hand, if oxidation or scaling is not diffusion controlled, but is wholly or partially dependent on interface reactions, then additional field effects of a somewhat different nature become possible.

Uhlig[7] has presented evidence to show that the slow step in the oxidation of many metals may be electron flow across the interface from the metal to oxide. The activation energy for oxidation then becomes directly related to the energy required for the transference of an electron from the metal to a physically absorbed O_2 molecule.

For oxidation reactions that are controlled by chemisorption at an interface, the state of electrical polarity of the surface can have a significant effect. It has been shown, for example,[8] that the rate of adsorption of O_2 on ZnO surfaces is accelerated when the oxide is positively polarized so that electrons are attracted to the surface, while desorption is enhanced at a negatively polarized surface.

B. THE USE OF ELECTRIC FIELDS TO CONTROL HOT CORROSION

In marine environments, high temperature turbine components are subject to a particularly insidious form of environmental degradation, known as hot corrosion. While the mechanism is incompletely understood, a condensed film of sodium sulfate, deposited onto the surface of the components, is supposed to be the major culprit responsible for the severe alloy deterioration that has been observed. The precise role of the sodium sulfate in bringing about the combined sulfur and oxygen attack which characterizes hot corrosion is unclear. However, work at United Aircraft Research Laboratories has suggested that the critical factor is the oxide ion activity of the melt.[9][10] Bornstein and

DeCrescente have shown[9] that certain oxides such as Cr_2O_3, V_2O_5, and MoO_3, can decrease the oxide ion activity of a Na_2SO_4 melt, with a significant decrease in over-all oxidation rate. It should also be possible to decrease oxide ion activity in the melt by maintaining the base alloy anodic. At an anode (positive electrode), oxide ions might tend to be destroyed.

$$O^{=} \longrightarrow \frac{1}{2} O_2 + 2e$$

In advanced marine turbine engines, the combustion gases are electrically conducting. Furthermore, ingestion of sea salt will greatly enhance the conductivity. Thus, it should be possible to sustain a current by applying a potential between a turbine component and an inert or sacrificial electrode elsewhere in the combustion zone. The primary objective of the experimental work described below is to investigate how such applied potentials might be used to control various steps of the hot corrosion mechanism.

In a molten Na_2SO_4 salt bath, clear evidence (see Figure 2) has been obtained for anodic protection of Ni-20 Cr alloys above a current threshold which depends on the precise nature of the alloy. The results in Figure 2 show that both anode and cathode are severely corroded up to a current level of 0.83 milliamps/cm^2. At 1.39 milliamps/cm^2, anodic protection is evidenced, particularly at the air/molten salt interface. At 1.67 milliamps/cm^2, the anode is virtually unattacked, while the cathode is severely corroded. Although it is not apparent in the photographs, corrosion is accompanied by extensive delamination, suggesting attack at edges and corners. The anodic protection is observed with both an active cathode of Nichrome and an inert cathode of platinum.[11] Similar results were reported by Simons, Browning, and Liebhafsky[12] for stainless steel. When a potential of 45 volts D.C. and a current of 0.1 amp was applied across two 310 stainless steel electrodes, partially immersed in molten Na_2SO_4, the cathode was almost totally destroyed by corrosion, while the anode was virtually unattacked. To the extent that hot corrosion in flames is similar to molten salt corrosion, a similar type of anodic passivation might be expected.

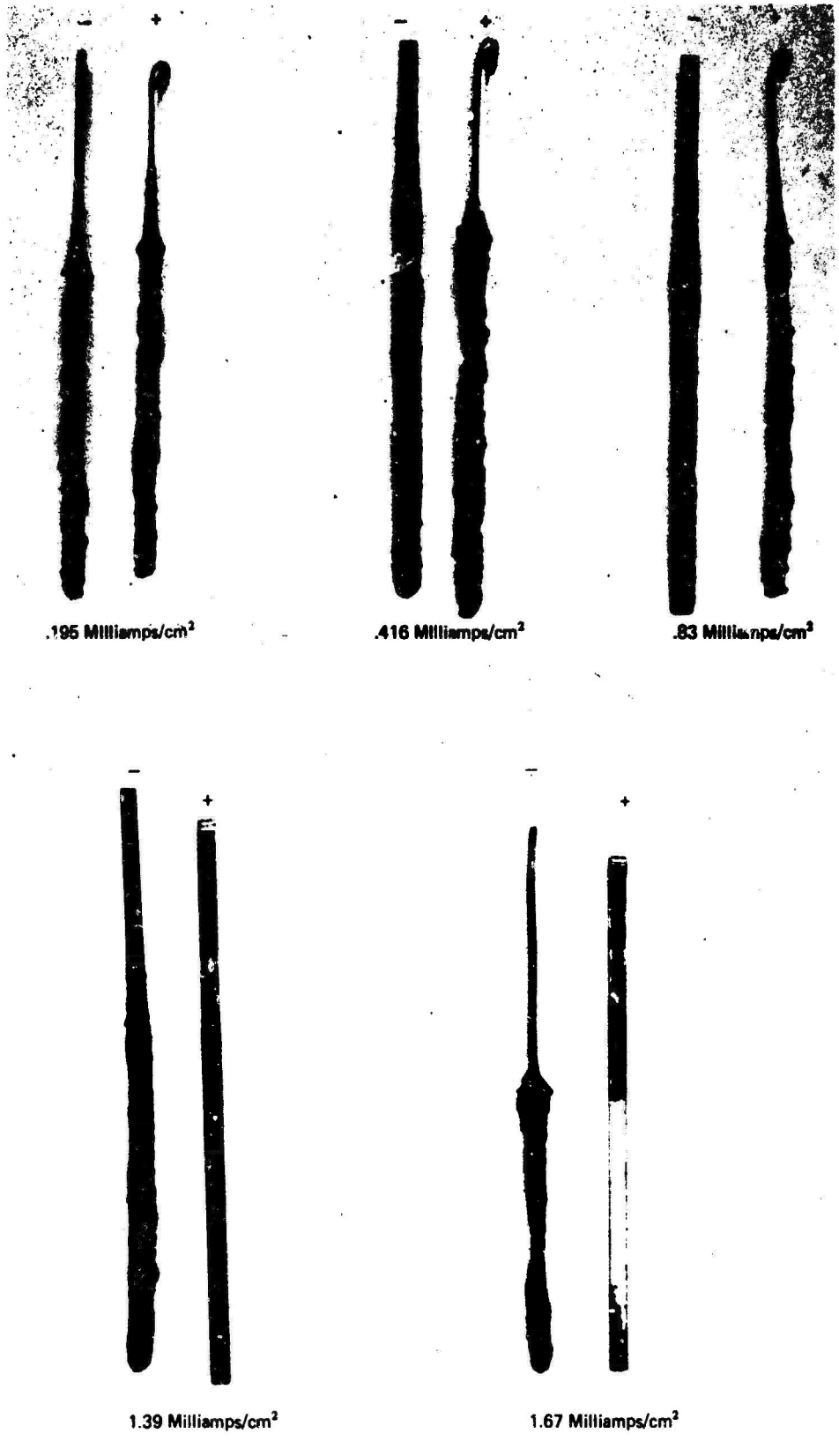

FIGURE 2. EFFECT OF CURRENT DENSITY AND THE CORROSION OF NICHROME IN MOLTEN SODIUM SULFATE AT 900°C

II. TEST PLAN AND EXPERIMENTAL PROCEDURE

A. MOLTEN SALT TESTS

The apparatus used for the molten salt tests is shown schematically in Figure 3. The salt is contained in a Vycor crucible, which in turn is inserted into a Cenco-Cooley electric furnace. Temperature is measured with a chromel-alumel thermocouple immersed in the molten salt. The cover of the furnace is a transite board with holes drilled for the sample electrodes and thermocouples. Temperatures were in the range 900-950°C. The atmosphere above the melt was air. The applied voltage varied from 0 to about 2.5 volts, and the corresponding currents were in the range 1-10 milliamps/cm^2.

B. CORROSION BURNER RIG TESTS

The apparatus used for the flame tests is shown schematically in Figure 4. It consists of a refractory lined furnace, a flame exit work area with a water-cooled outer electrode shield, and an inner or working electrode. The walls of the furnace are insulated with Babcock and Wilcox Kaowool castable insulation so that the inner furnace wall is maintained at as high a temperature as possible (about 1300°C) to minimize condensation of the salt used for flame seeding.

A propane/air mixture is fed at a ratio of 1 to 20.68 by a series regulator-flow meter system for both the air and fuel streams. The seeding solution of 80 g/l of sodium sulfate salt in water is pulse-injected into the furnace tangential to the gas flow at 5 ml/min, giving a salt concentration in the flame of about 1850 ppm.

The electrode configuration described above was selected so as to provide a large surface area for the outer reference electrode with respect to the inner electrode, and hence to assure that electrical characteristics were controlled by the inner electrode. In earlier work two strip electrodes were exposed simultaneously, with the potential applied between them. Temperatures were measured with an optical pyrometer.

Working electrodes of several configurations were tested. Early experiments were done with Nichrome strip electrodes, but observations of arcing off the edges of the samples suggested the presence of inhomogeneities in the electric field. Furthermore, the flame itself has a noticeable vortex-like motion. To minimize the influence of these extraneous factors on the results, we did an extensive series of tests with suspended spherical Inconel 600 electrodes. It was hoped that the spherical geometry would eliminate the obvious edge effects noticed previously which seemed to be the point of initiation of corrosion. By providing a uniform spherical surface the erratic onset of corrosion might be eliminated and a more uniform corrosion growth might be experienced which would provide a more consistent corrosion growth rate.

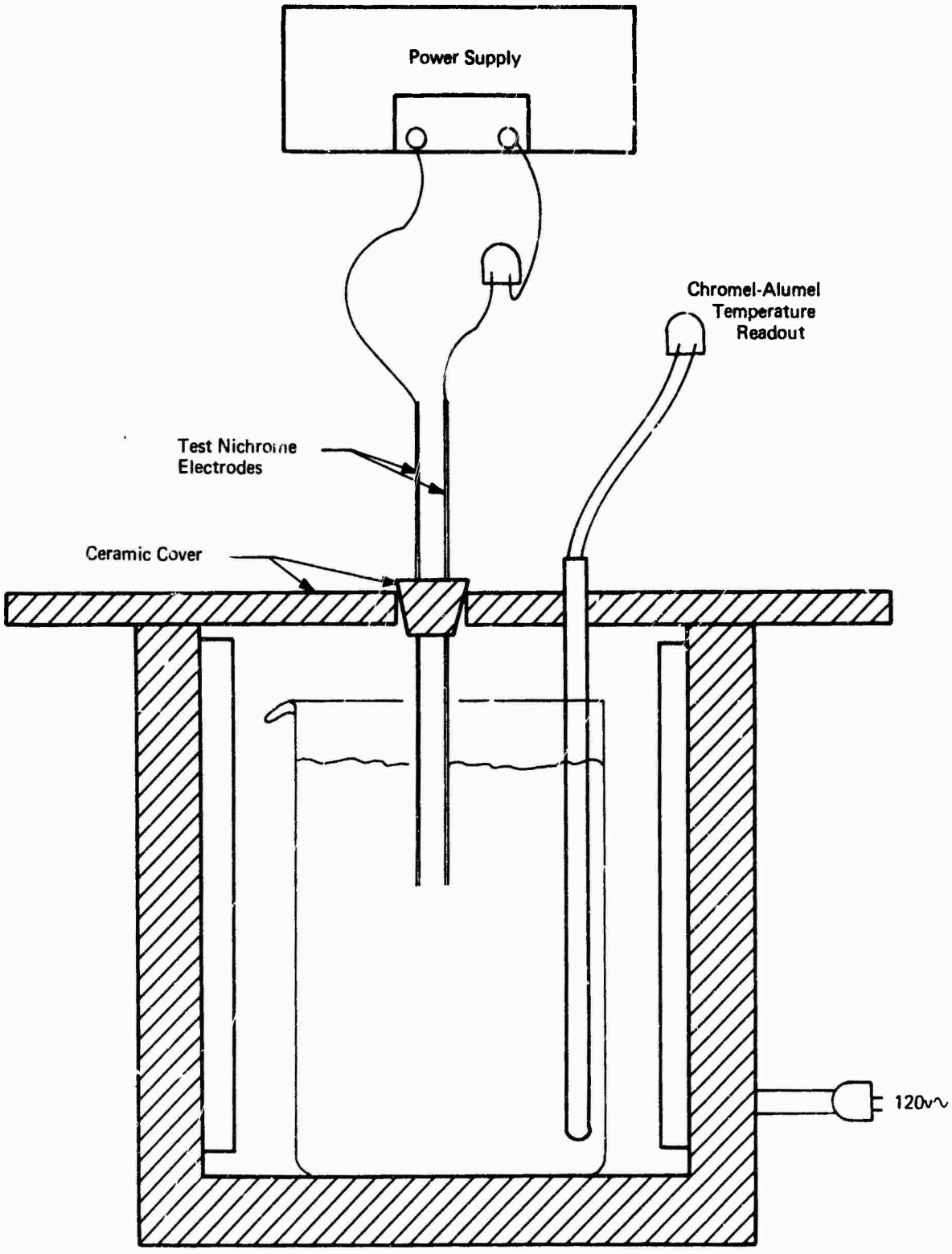

FIGURE 3 MOLTEN SALT BATH IN ELECTRICAL RESISTANCE FURNACE

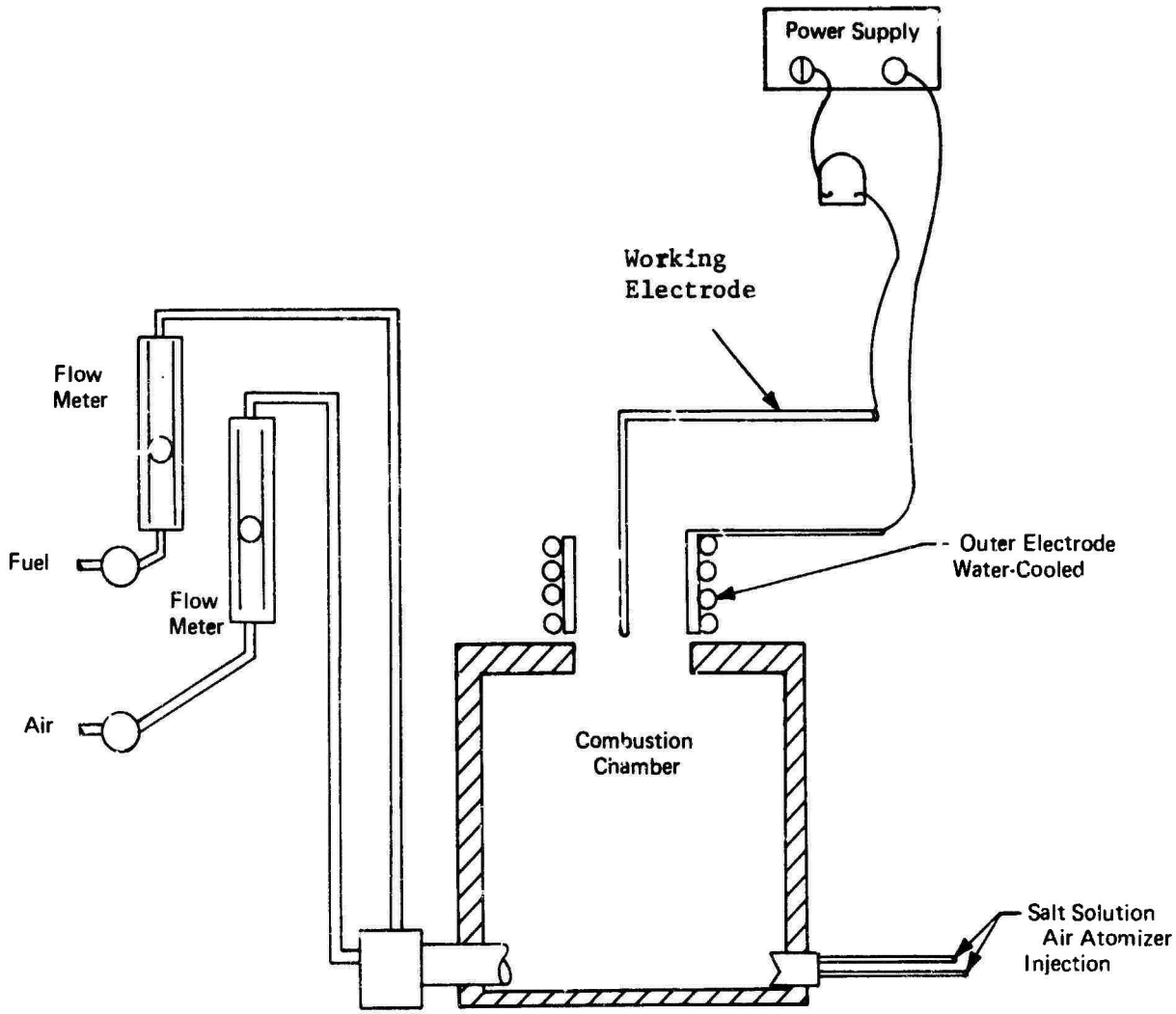

FIGURE 4 APPARATUS TO STUDY THE EFFECT OF ELECTRIC FIELDS ON CORROSION IN SALT SEEDED FLAMES

A test configuration for the shperical electrodes is shown in Figure 5. The sample to be tested is prepared by attaching a wire lead by electric discharge techniques; the join area is subsequently protected by a small ceramic cover. In some instances, a multiple ball test was found to be instructive and a multiple ball array tester was developed for this purpose. The electronics for providing different voltages and different currents to a seven-ball test array is shown in Figure 6.

C. SAMPLES

Experiments were carried out using the following types of samples:

Electrode	Configuration
Nichrome	strip
Inconel 600	spherial
Nickel	cylindrical
Hastelloy X	strip
Co-25 Cr-6 Al-0.1 Y	strip

The configurations were dictated largely by the availability of material. Test on nickel, Inconel 600, Nichrome, and Hastelloy X were run to obtain some understanding of the effects of alloying elements on the hot corrosion of nickel based chromium oxide forming alloys under the influence of an electric field. The CO-Cr-Al-Y alloy was studied to explore the effects of an applied electric field on an aluminum oxide forming high temperature material.

D. TEST PROCEDURE

A major part of the test program focused on corrosion tests in the flame with spherical balls, formed from bar stock of Inconel 600. These tests were performed at temperatures between 925°C to 950°C. In some cases, the current to the spherical sample was controlled at a constant level while in other cases, voltage was controlled.

Two methods of analysis were used to establish the amount of corrosion experienced by the spherical samples during a test. A macroscopic weight analysis method was developed which depends on a de-scaling technique. For a more detailed analysis of the type and extent of corrosion, metallographic techniques and x-ray probe analysis were also used, however on a smaller number of samples.

The de-scaling method utilizes an acid mixture which removes the corrosion zone from the spherical ball without any noticeable effect on the original material. The remaining uncorroded part of the spherical sample is then weighed and the weight ratio to its original weight represents the amount of uncorroded material. The acid mixture consists of: 90 ml water, 30 ml H_2SO_4, 30 ml HNO_3, 30 ml glacial acetic acid. The mixture is heated to about 120°C and the sample to be descaled is immersed. Within seven minutes, the activity at the sample surface subsides and the scale has been removed.

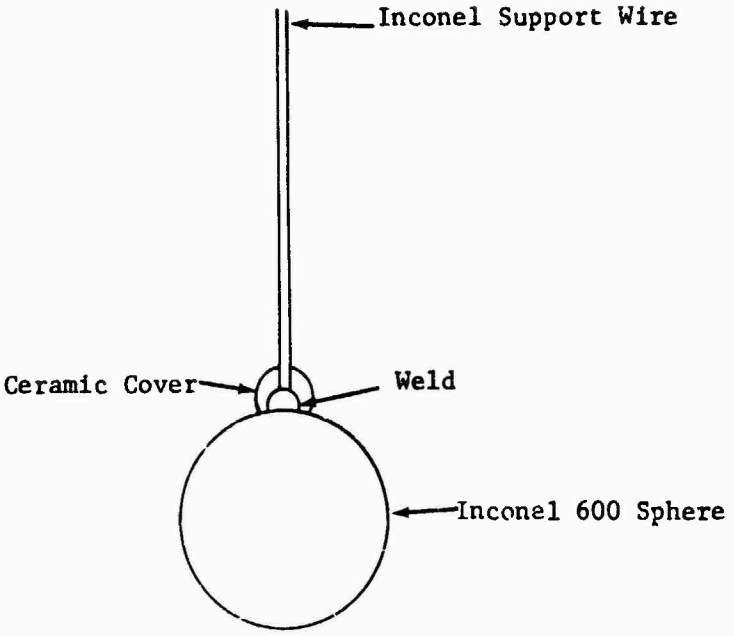

FIGURE 5
INCONEL 600 Spherical Electrode

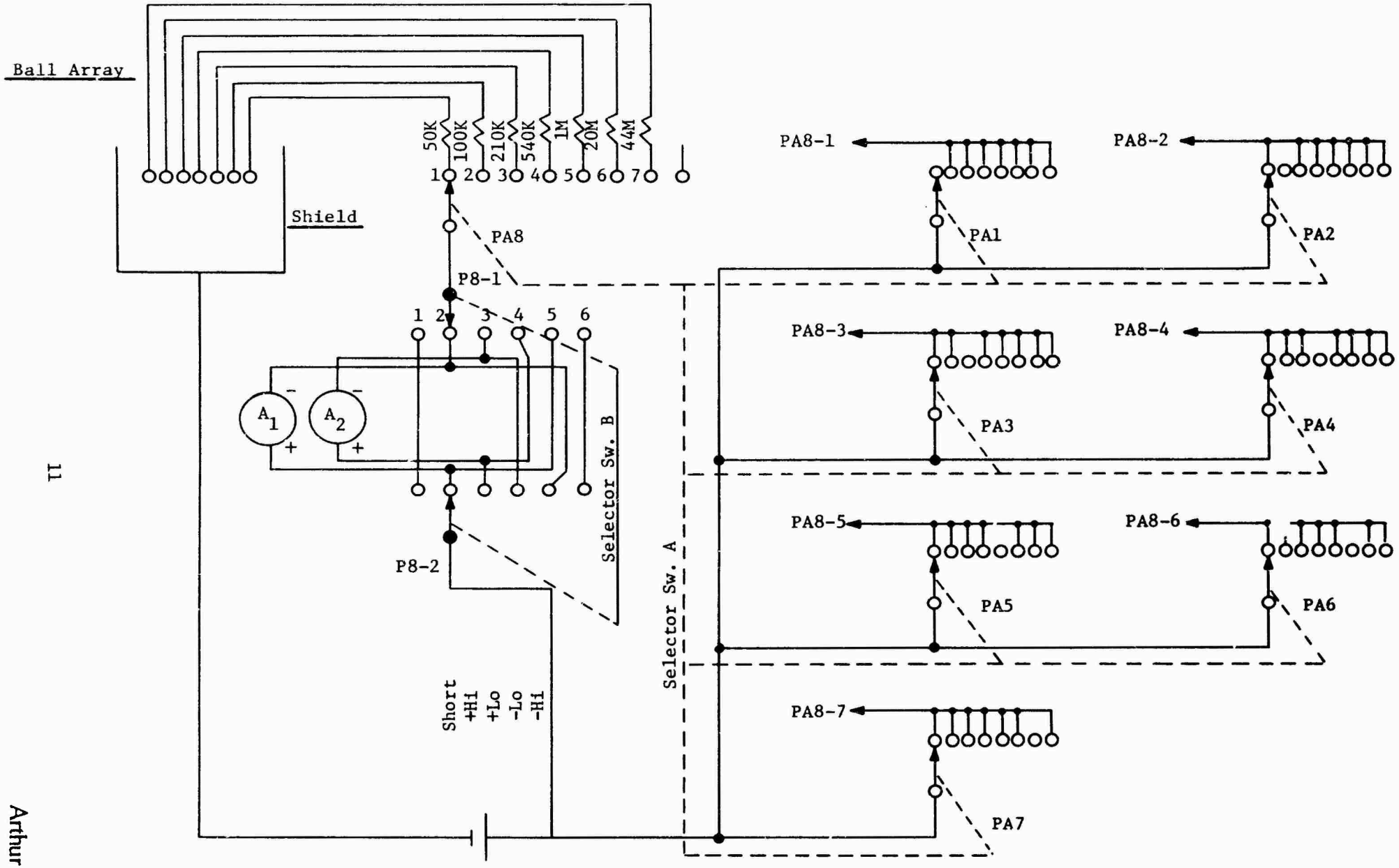

FIGURE 6

7-SAMPLE ARRAY TESTER

Several spherical samples were mounted and cross sectioned for metallographic analysis. X-ray probe analysis revealed the nature and amount of reaction at the interface of the original metal and the oxide zone.

III. EXPERIMENTAL RESULTS

A. MOLTEN SALT TESTS

Twenty-two molten salt tests with nichrome strip samples were performed to verify the effect of applied electric fields on corrosion in molten salt baths. The experimental conditions are summarized in Table 1 and results are plotted in Figure 7. Examination of paired exposures in Table 1 shows, with a single exception, that corrosion levels of cathodically polarized samples are 1.3 to 7.3 times greater than those of anodically polarized samples.

Additional molten salt bath tests were performed with spherical samples of Inconel 600. In the tests summarized in Table 2, the Inconel spheres were held with Inconel wire electrically discharged welded to the spheres. In some cases the weld was the site of intensive corrosion and the Inconel 600 sphere was lost to the melt. In other cases, the wire was severely corroded and the results were thought to be biased by the corrosion of the suspension wire rather than the spherical sample. A new set of tests was performed with a platinum wire attached to the Inconel spheres. These are shown in Table 3 with samples #9 - 29. The results of these samples tested for two hours' exposure are shown in Figures 8 and 9.

Preliminary tests with Inconel 600 spherical samples showed that no corrosion occurred when they were submerged in sodium sulfate molten salt, in marked contrast to results with rectangular strip samples. It was found that corrosion could be induced in the spheres, however, if the smooth spherical surface was slightly abraded mechanically. The small indentations formed in a mechanical vise provided sites from which corrosion could be initiated. Such roughened balls proved to be affected by applied current in the molten salt, but in a different way from the strip samples. Shown in Figure 8 is the summary of molten salt bath tests on Inconel 600 spheres. The data are displayed on semi-logarithmic paper. The results shown in Figure 8 are those tests in which the final current was obtained by adjusting upward from zero to the fixed test current shown on the abscissa. Similar data are shown in Figure 9 in which the current was adjusted from a high value down to the set current. The difference in the data reported in Figures 8 and 9 is a shift in the profile of the corrosion versus current curve. In Figure 8, where current was adjusted upward, the region of essentially zero corrosion extends from about -0.6 to +3.0 milliamps/cm^2. In Figure 9, where the current was adjusted downward, the region of zero corrosion was compressed to the range -0.1 to 0.5 milliamps/cm^2. Thus, the onset of corrosion may be initiated by the initial application of sudden high currents.

Hastelloy X strip samples immersed in the molten salt bath under the conditions given in Table 4 corroded very extensively and to approximately the same extent on both the anodic and cathodic sides in each pair of exposures. The fact that Hastelloy X oxidizes below 980°C to form a surface layer of amorphous silica[16], while Inconel 600 is a chromia former may account for the differences.

TABLE 1

MOLTEN SALT BATH - NICHROME STRIP SAMPLES
(all 1 hour exposure)

Apparatus - Figure 3

Sample	Volts (E)	Current in Milliamps	% Corrosion + Side (anode)	% Corrosion - Side (cathode)	Ratio of Corrosion, - Side / + Side
1	2.25	300			
2	2.25	300	Cathode corroded		
3	2.25	300	through; anode		
4	2.25	300	not measured		
5	2.25	300			
6	1.8	150			
7	1.8	150	6.79	34.2	5.04
8	1.8	150	7.70	21.9	2.84
9	1.8	150	16.3	10.5	.64
10	1.93	200			
11	1.52	50	10.0	21.2	2.12
12	1.45	25	10.4	21.6	2.08
13	1.45	25	16.2	21.2	1.31
14	1.52	50	10.4	28.1	2.70
15	1.63	100	11.4	30.6	2.68
16	1.80	150	8.03	35.6	4.43
17	1.96	200	9.26	57.8	6.24
18	2.10	250	9.33	68.50	7.34
19	Floating		10.1		
20	Floating		10.8		
21	2.10	250	12.0	30.0	2.5
22	1.80	150	10.3	21.1	2.05

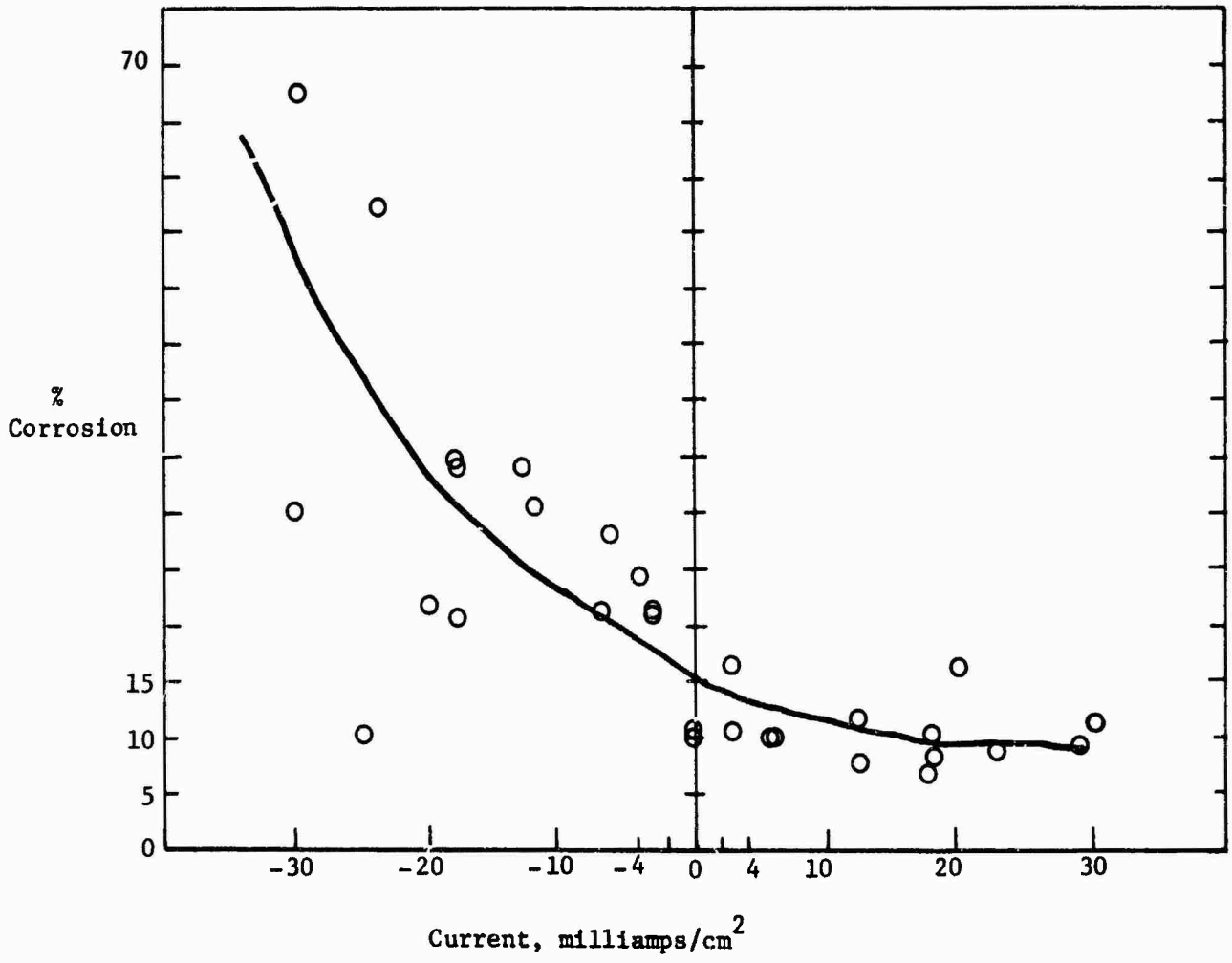

FIGURE 7

CORROSION VS APPLIED CURRENT FOR NICHROME STRIP SAMPLES

TABLE 2

MOLTEN SALT BATH - INCONEL 600 SPHERICAL SAMPLES - Inconel Wire
(all 1 hour exposure)

Sample	Current (I) (milliamps)	% Corrosion	
		anode	cathode
1 C	0	0	0
3 C	25	0	19
4 C	5	Lost Ball in Melt	
5 C	10	15.8	0.5
6 C	5	0	0
7 C	12 to 15	0	0

TABLE 3

MOLTEN SALT BATH SPHERICAL INCONEL 600 SAMPLES - Platinum Wire
(2 hour exposure)

Sample No.	Current in Milliamps	% Corrosion	
		Anode	Cathode
9 C	5.0	1.8	31.3
10 C	1.0	0.6	22.5
11 C	10.0	2.0	2.0
12 C	10.0	4.7	27.2
13 C	20.0	10.7	30.4
14 C	0.5	0.0	31.3
15 C	0.0	0	0
16 C	0.0	0	0
17 C	0.1	0	0
18 C	0.05	0	0
19 C	2.0	0.4	13.4
20 C	.25	0	0
21 C	.40	0	0
22 C	.35	0	0
23 C	.45	0	0
24 C	.70	0	0
25 C	3.5	0	1.2
26 C	7.0	3.1	7.0
27 C	10.0	2.0	24.0
28 C	50.0	8.2	--
29 C	100.0	--	14.7

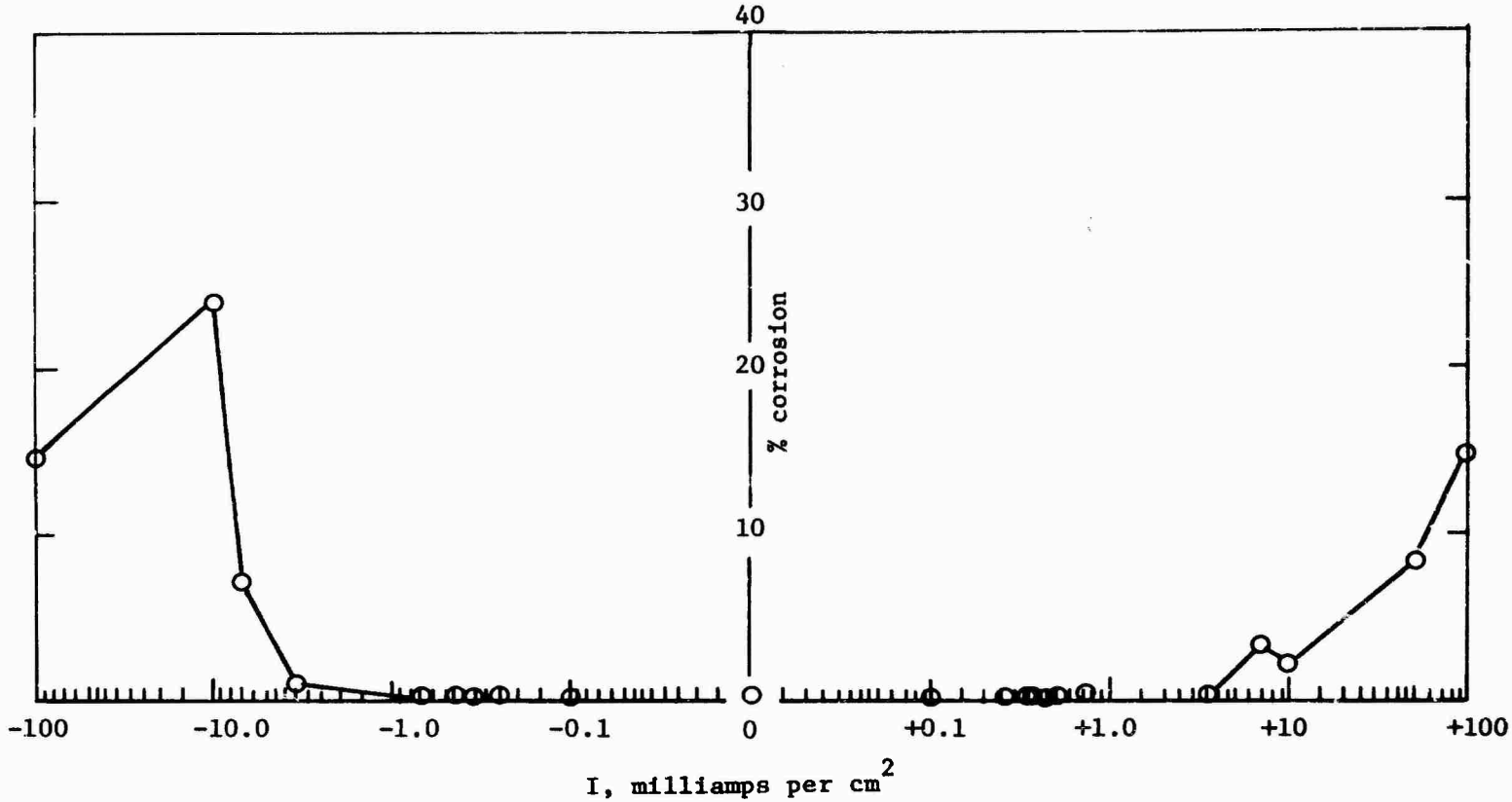

FIGURE 8

CORROSION VS APPLIED CURRENT FOR INCONEL 600 SPHERES IN MOLTEN Na_2SO_4
(current - adjusted upward from 0 to the value indicated)

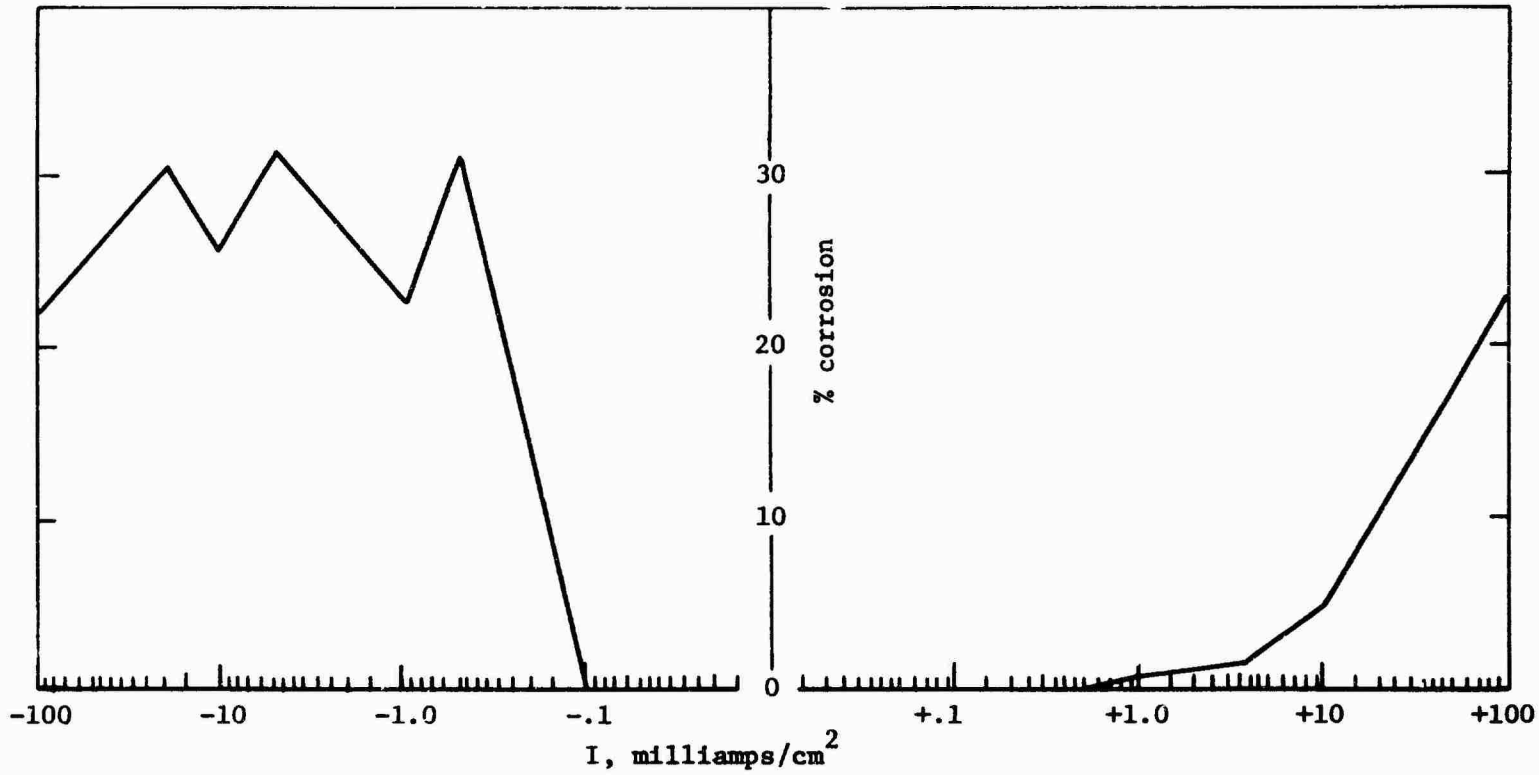

FIGURE 9

CORROSION VS APPLIED CURRENT FOR INCONEL SPHERES IN MOLTEN Na_2SO_4

(current - adjusted downward to the value indicated, at set up)

TABLE 4

MOLTEN SALTS

Hastelloy X Strip

Sample	Current in milliamps	Exposure
1	100	30 minutes
2	100	15
3	50	15
4	100	5
5	100	1
6	50	1
7	25	1

B. FLAME TESTS

In the molten salt bath tests, strong anodic protection was observed for nichrome strip samples, and a long region of essentially zero corrosion was observed for Inconel 600 sphere samples at both low anodic and low cathodic currents. If hot corrosion in flames is initiated by condensation of a thin film of molten sodium sulfate on the surface of the sample, then application of an electric field might effect the rate of corrosion in a manner similar to that observed in the molten salt.

1. Inconel 600 Spheres

Four series of flame tests with Inconel 600 spherical samples were performed and are shown in Tables 5 and 6 and Figures 10-13. Each test was done with a single propane tank. Grouping together test runs made with the same propane tank is a precautionary measure arising from the concern that small variations in amounts of trace components in the propane bottles could affect the rate of corrosion. Subsequent mass spectrometric analysis of propane showed that a fairly large fraction (5%) of the gas drawn from the last of the tank contents was butane plus hydrogen sulfide. These two components could cause a reduction in the flame temperature and a change in the flame chemistry. Therefore in each test set the tests were terminated before the propane bottle was more than 50% empty in order to prevent the heavy gaseous components from entering into the experiment.

In each of the four tests the current level was gradually increased and the exposure time was maintained at two hours except for a few instances in which a single hour test was performed to check the time dependence of the corrosion growth rate.

In the first set of tests small positive and negative currents were applied to the spherical samples to determine the effect of electric field in and around zero microamps.

Corrosion appeared to be a minimum at a very slight positive current, as shown by a repeated drop in corrosion close to +10 microamps per sq. centimeter at the working electrode (see Figures 10 and 11). However, repeated efforts at confirming that corrosion was indeed a minimum in a small microamp positive range proved to be difficult since variations in the propane tank appeared to give substantial differences in the amount of corrosion.

In tests 4/27/1, 4/27/2, and 5/3/ (Table 5), a small negative current was measured when the sample and counterelectrode were shorted together. This is discussed in the previous year's work[11] and is a phenomenon common in all flames due to the high electron mobility which dominates the flame, biasing the species incident on a sample with negative charges. Therefore it may be expected than when the electrode and counterelectrode are shorted together a negative bias current is experienced on the hotter test electrode.

TABLE 5

INCONEL 600 SPHERE

FLAME TESTS

Set 1

Sample Identification	Volts	Current, Microamps	Temp.°C	Exposure Time, hours	% Corrosion
5/7/	0	NA	890	2	3.3
5/4/1	0	NA	900	2	0
4/27/1	0	5.5	890	2	19
4/27/2	0	4.8	885	2	25
5/3/	0	.5	905	2	43.2
5/1/1	+1.25	0	895	2	29.1
5/1/2	+1.51	0	850	2	17.5
4/31/	+10.0	45	885	2	18.2
5/4/2	25.	80	900	2	0.19
			New Propane Tank		
5/16/	NA	0	895	2	27.8
5/17/1	NA	0	895	2	21.7
5/19/	NA	0	880	2	21.6
5/14/1	-1.5	4	908	2	31.
5/21/1	-1.5	4	900	1	15.1
5/9/1	-3.0	5	890	2	17.5
5/18/1	-4.0	6	902	2	21.6
5/22/	-10	10	905	1	15.1
5/9/2	-8	16	900	2	23.2
5/11/1	-20	30	900	2	27.7
			New Propane Tank		
5/22/1	0		905	1	20.0
5/22/2	-500	50	900	1	13.5
5/21/2	+ .7	4	905	1	10
5/17/2	+ .9	6	910	2	23.8
5/18/	+ .9	6	903	2	19.2
5/17/3	+1.5	10	905	2	24.0
5/18/2	+1.5	15	900	2	27.7
5/17/4	+1.0	15	906	2	28.5
5/14/2	+5.0	20	905	2	27.7
5/11/2	+7.5	30	900	2	25.0
5/11/3	+8	30	900	2	27.7
5/14/3	+10	50	900	2	26.3
5/23/1	+12	40	906	1	13.4
5/23/2	+20.5	70	910	1	19.7
5/23/3	+67.3	200	909	1	17.7
5/22/2	+500	800	905	1	14.9

TABLE 5 (Cont.)

Sample Identification	Volts	Current, Microamps	Temp.°C	Exposure Time	% Corrosion
5/23/4	-460	40	910	1	18.6
5/23/5	-200	20	905	1	16.6
5/23/6	-120	10	905	1	15.6
6/8/1	NA	0	890	1	8.6
6/11/1	NA	0	902	1	15.7
6/8/2	+ .2	5	905	1	1.6
6/11/2	-	5	905	1	0.3
5/23/4	+ 2.38	10	910	1	13.1
6/11/3	+ 2.7	15	905	1	15.4
6/8/1	+ 4.0	15	905	1	14.6
5/23/5	+ 6.6	25	905	1	14.3
6/11/4	+ 4.2	30	905	1	15.4
6/11/5	+11.6	60	905	1	0.4

TABLE 6

INCONEL 600 SPHERES

FLAME TESTS, Set 2

One Hour Exposure

Sample Identification	Volts	Current, Microamps	Temp. °C	% Corrosion
6/27/1	0	0	915	17.4
6/27/2	0	0	910	0.6
7/26/1	0	0	902	13.1
7/27/1	0	0	900	10.7
7/27/2	0	0	900	13.9
8/6/1	0	0	910	16.0
8/7/1	0	0	912	14.9
7/27/3	-.65	1	900	12.0
7/27/4	-.30	2	900	11.0
7/27/5	-.03	3	902	9.2
7/27/6	+.34	4	900	11.0
7/26/2	.3	5	910	13.0
8/7/2	.67	5	900	7.4
8/1/1	6.5	6.5	895	10.8
8/1/2		9.7	895	11.3
7/26/3	1.4	10.0	910	13.9
6/27/1	1.37	10.0	902	15.1
8/7/3	1.69	10.0	910	13.1
8/6/2	7.9	15	895	14.7
8/1/3	5.3	15	890	8.0
7/26/4	4.5	20	910	13.0
6/27/2	3.0	20	902	14.6
8/6/3	6.3	25	900	11.2
8/6/4	9.9	35	910	15.3
7/26/5	15.0	50	910	13.0
6/27/3	15.0	50	910	15.0
8/6/5	23.6	75	910	14.7
8/1/4	35.3	100	895	12.8
8/6/6	32.3	100	910	16.3
8/7/4	300	900	900	15.2
8/7/5	500	1100	902	14.7
8/7/6	750	1500	905	15.0

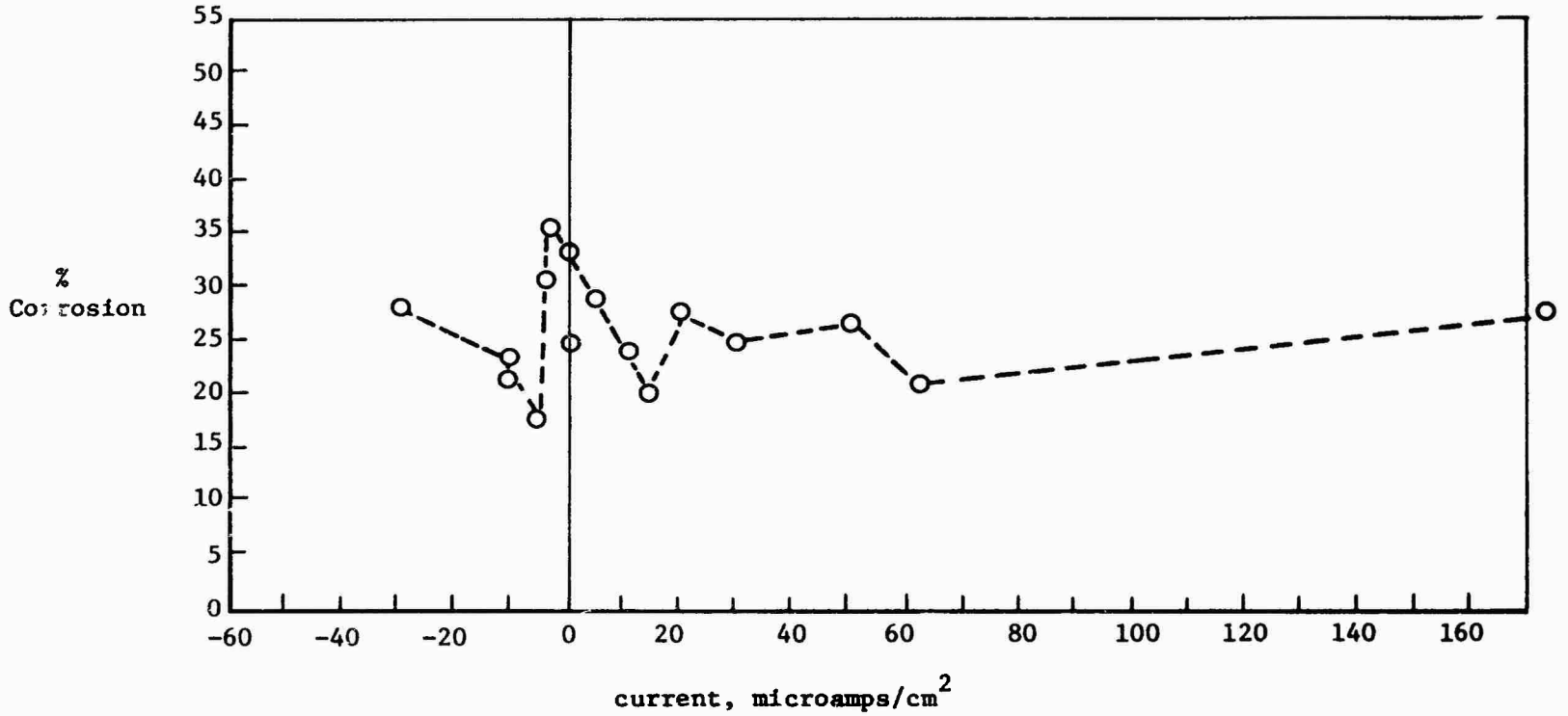

FIGURE 10

CORROSION VS CURRENT AT THE WORKING ELECTRODE - INCONEL 600 SPHERES IN Na_2SO_4 SEEDED FLAMES

(Series #18-35)

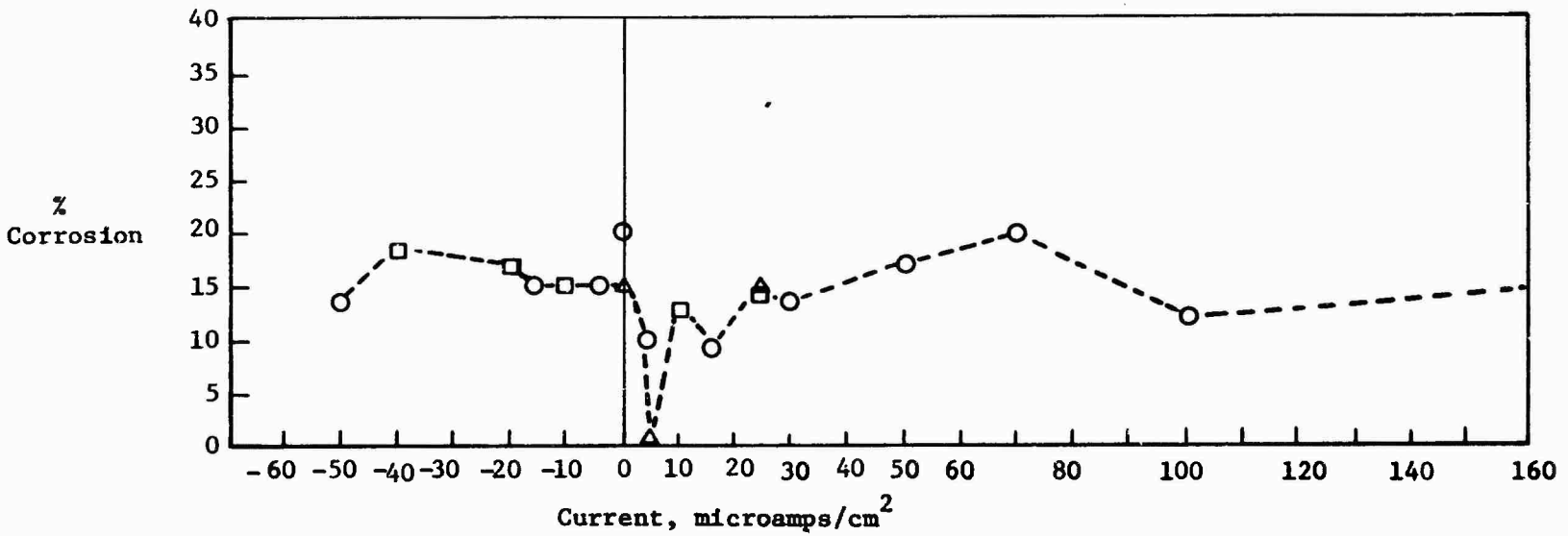

FIGURE 11
CORROSION VS CURRENT AT THE WORKING ELECTRODE - INCONEL 600 SPHERES IN Na_2SO_4 SEEDED FLAMES

(Series #47-63)

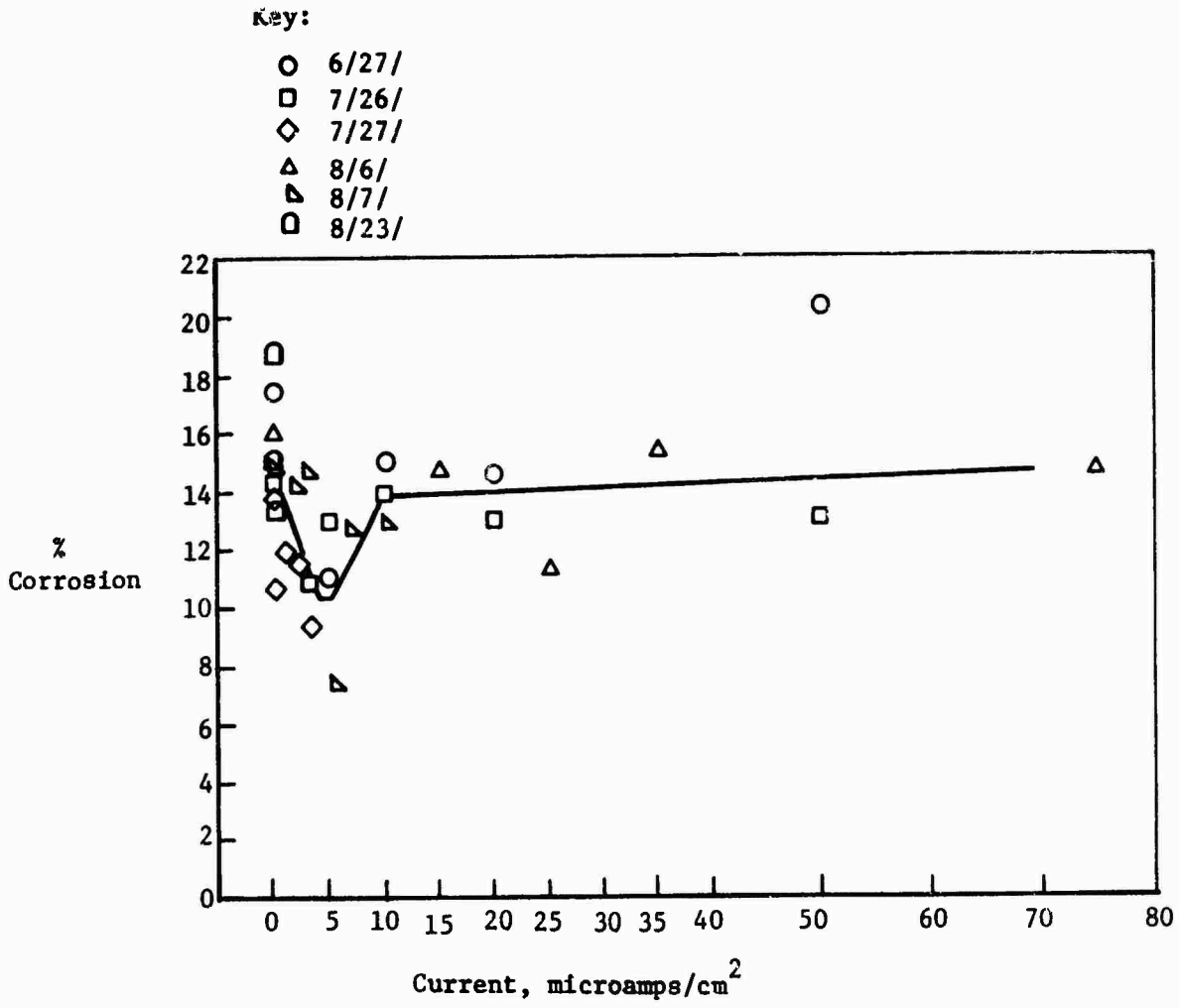

FIGURE 12

SECOND SET OF INCONEL 600 SPHERE FLAME TESTS

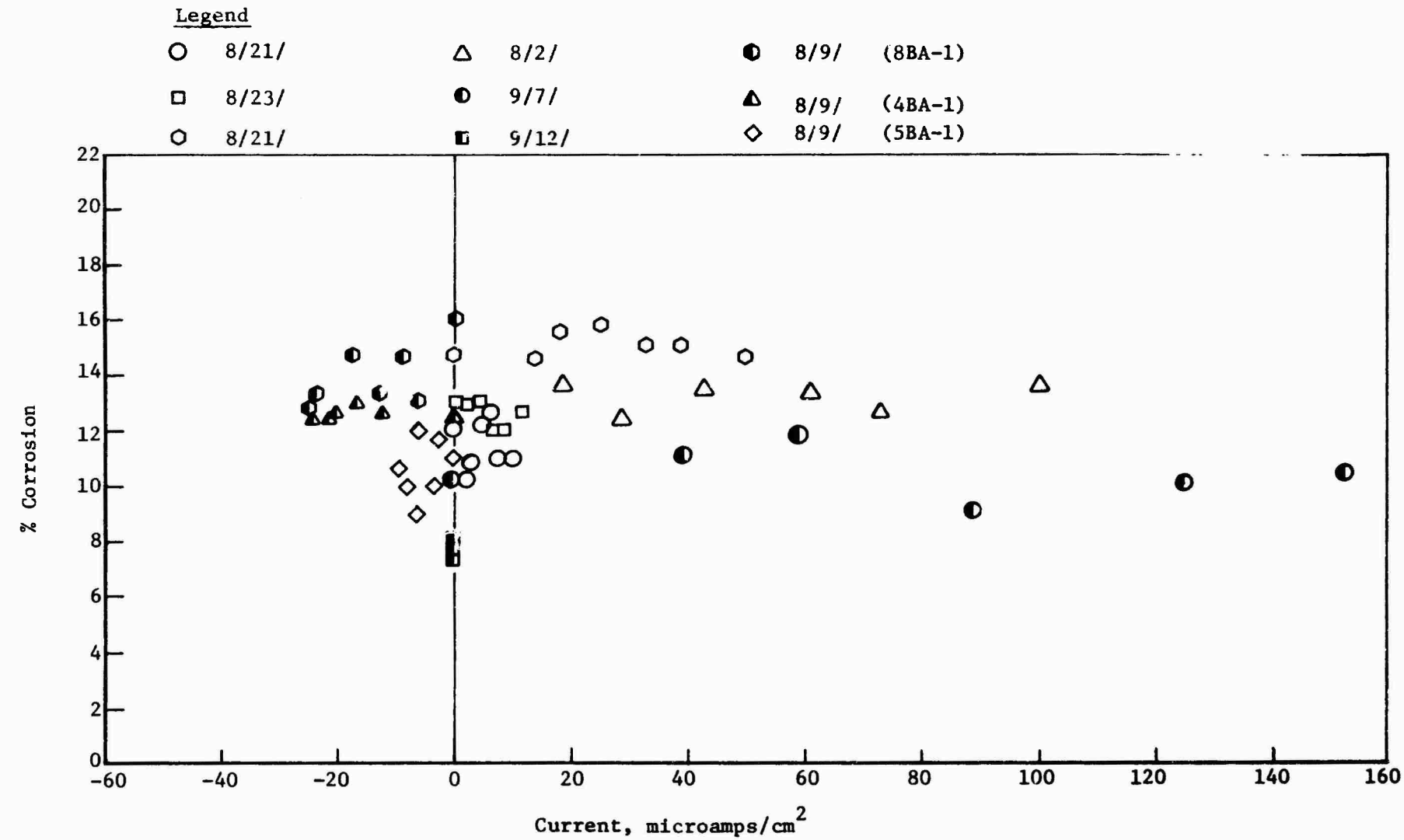

FIGURE 13

7-BALL TEST SUMMARY

The second set of tests consisted of single-hour exposures and showed that corrosion in the salt-seeded flame proceeds with a near linear growth rate; i.e., half the exposure time results in approximately half the corrosion, as shown in Table 5 and Figure 12.

To eliminate possible effects of deviations in gas composition on corrosion rates, a series of one hour tests was carried out with high purity propane gas. Once again a small reduction in corrosion was observed at small positive currents, similar to that found in the previous sets of experiments. It was concluded that the impurities in the propane from the commercial grade while affecting corrosion on a gross scale by reducing the flame temperature did not appreciably affect the corrosion behavior in the presence of an applied electric field.

Many tests were performed without an applied electric field (0 microamps). These tests show a wide variation in percent corrosion. In contrast, the percent corrosion observed in the presence of an applied electric field seemed to be far more repeatable and uniform. This suggests that the applied field, apart from an effect on the chemical reaction, does affect the physical environment of the sample. The applied field might in essence produce a more uniform distribution of some species in the vicinity of the electrode.

In order to eliminate the variation of flame dynamics and conductivity which may be experienced by sequential testing of samples, twelve tests with Inconel 600 spheres were performed with the seven sample tester discussed earlier which permitted the simultaneous exposure of seven samples to different currents in the same flame. Results are shown in Table 7 and summarized in Figure 13.

The variation in amount of corrosion in any seven ball test is within the expected experimental accuracy of the test indicating a uniform corrosion with each seven ball test. Variability between seven ball tests indicates no significant trends which can be linked to the effect of an electric field on corrosion. The average levels of corrosion fall between 7.6% and 15.2%, and do not correlate well with either temperature or current density.

The seven ball array appears to wash out variations between samples in the levels of corrosion. In the test of floating samples no substantial corrosion variations between samples was observed. The effect of adding seven spheres to the flame reduces the free cross section available to gas flow and increases mixing of the gaseous in the flame. Furthermore, the addition of a field of thermally conductive electrically charged material (Inconel 600 spheres) in the flame as the effect of stabilizing premixed flames. Powling and Egerton[13] use a wire gauze for stabilization of flame edge as well as providing a uniform flow pattern. Flame

TABLE 7

FLAME TEST - MULTIPLE SPHERES
(1 hour exposure)

Sample	Current, Microamps/cm^2	Voltage	Temp. °C	% Corrosion	
73-7BA-1	Floating		920	12.1	
-2	10.0	4	920	11.0	
-3	7.4	3.5	920	11.0	
-4	6.1	3.0	935	12.7	Average 11.3 ± 1.25
-5	4.3	2.0	935	12.2	
-6	3.0	1.5	940	10.8	
-7	2.1	1.0	940	10.2	
73-9BA-1	Floating		950	13.0	
-2	11.9	4	950	12.7	
-3	8.8	3.5	950	12.0	
-4	7.0	3.0	950	12.0	Average 12.5 ± .5
-5	4.7	2.0	948	13.0	
-6	3.0	1.5	950	12.9	
-7	2.1	1.0	955	12.9	
73-6BA-1	Floating		910	14.7	
-2	+50	25	910	14.7	
-3	+39.0	20.5	938	15.1	
-4	33.0	17.5	950	15.1	Average 15.2 ± .6
-5	25.0	15.	950	15.8	
-6	18.0	13	938	15.6	
-7	14.0	10	922	14.6	

TABLE 7 (Cont.)

Sample	Current, Microamps/cm^2	Voltage	Temp. °C	% Corrosion	
73-3BA-1	100	75	910	13.6	
-2	73	57.0	910	12.7	
-3	61	47.5	920	13.4	Average
-4	43	31.0	908	13.5	13.0 ± .65
-5	29	25.0	905	12.4	
-6	19	20	910	13.7	
73-11BA-1	Floating		940	10.2	
-2	203	150	928	10.4	
-3	152.0	115	942	10.4	
-4	125.0	90	950	10.0	Average
-5	88.8	60	950	9.1	10.0 ± 1
-6	59.0	43	948	11.8	
-7	39.2	30	948	11.1	
73-12BA-1	Floating		950	7.2	
-2	Floating		950	7.2	
-3	Floating		942	8.1	
-4	Floating		942	7.2	Average
-5	Floating		950	7.2	7.65 ± .45
-6	Floating		932	7.6	
-7	Floating		950	7.3	
73-8BA-1	Floating		928	16.0	
-2	-25	150	932	12.8	
-3	-23.3	120	938	13.3	
-4	-17.7	90	938	14.7	Average
-5	-12.9	60	945	13.3	14.6 ± 1.4
-6	- 8.7	45	945	14.7	
-7	- 6.5	20	940	13.1	

TABLE 7 (Cont.)

Sample	Current, Microamps/cm^2	Voltage	Temp. °C	% Corrosion	
73-4BA-1	Floating		910	12.5	
-2	-24.5	100	910	12.4	
-3	-23.9	96	912	12.4	Average 12.7 ± .3
-4	-21.2	86	922	12.4	
-5	-20.8	80	922	12.6	
-6	-16.7	55	908	13.0	
-7	-12.8	10	908	12.7	
73-5BA-1	Floating		910	11.1	
-2	- 9.8 A	20	910	10.6	
-3	- 8.0	17	925	10.0	
-4	- 6.7	13	935	9.0	Average 10.5 ± 1.5
-5	- 5.7	11	940	12.0	
-6	- 3.8	5	940	10.0	
-7	- 2.5	2	910	11.7	

gauze stabilization is a common practice in many ion-current studies because it provides a more uniform distribution of ion species.[14] The strong radiative coupling of the spherical balls tending to make the local temperatures uniform brings the ionic species more into thermal equilibrium and creates a more stable and evenly distributed state which could contribute to the uniform corrosion found in the seven ball tests.

In light of the small current levels of the tests the effect of the applied electric field is not expected* to dominate and the level of corrosion is seen to be nearly constant for the balls and dominated by the flame uniformity.

Although no striking effects of applied fields on the degree of corrosion of Inconel 600 spheres were observed, the descaling technique used would only reveal very gross macroscopic changes. Metallographic examination by optical and electron microscopy of nichrome strip samples exposed at 900°C for two hours at +500 and -500 volts suggest that there is a fundamental difference in the corrosion mechanism for anodically and cathodically polarized samples.

Photomicrographs of the cathodic and anodic samples are shown in Figure 14. The cathodic sample reveals a reaction zone about 5 mils in depth. Numerous precipitates are observed at the leading edge of this zone. The precipitates have both connected intergranular and spheroidal (1 - 3 μm in diameter) morphologies. In comparison, the reaction zone in the anodic sample is less than 1 mil in thickness, containing a large number of spheroidal (1 - 5 μm in diameter) precipitates.

Scanning electron micrographs and corresponding X-ray images of Cr, Ni and S are presented for the surface reaction layer of the cathodic sample in Plates 1 and 2 (both at 500X). The outer portion of the reaction zone (dark grey areas having a textured surface as observed in the micrographs) exhibits a high Cr intensity, with essentially no Ni or S. It is identified as Cr_2O_3. Substantial amounts of sulfur are observed along the interface between Cr_2O_3 particles and the metal matrix. These areas that are rich in Cr and S appear to be chromium sulfide particles. The other precipitates near the leading edge of the reaction zone are rich in S and contain some Cr. They are believed to be mixed chromium-alkali metal sulfides. The metal matrix in the reaction zone is almost completely depleted in chromium.

Results for the anodic sample are shown in Plate 3 (at 1000X) and Plate 4 (at 2000X). There is little indication of Cr_2O_3 particles in this sample. The grey precipitates observed in the micrographs are observed to contain Cr and S, and can be assumed to be chromium sulfide. The reaction zone matrix exhibits substantial depletion in chromium.

*As evidenced by the current density in milliamps per cm^2 necessary to halt scale growth in Molten Na_2SO_4

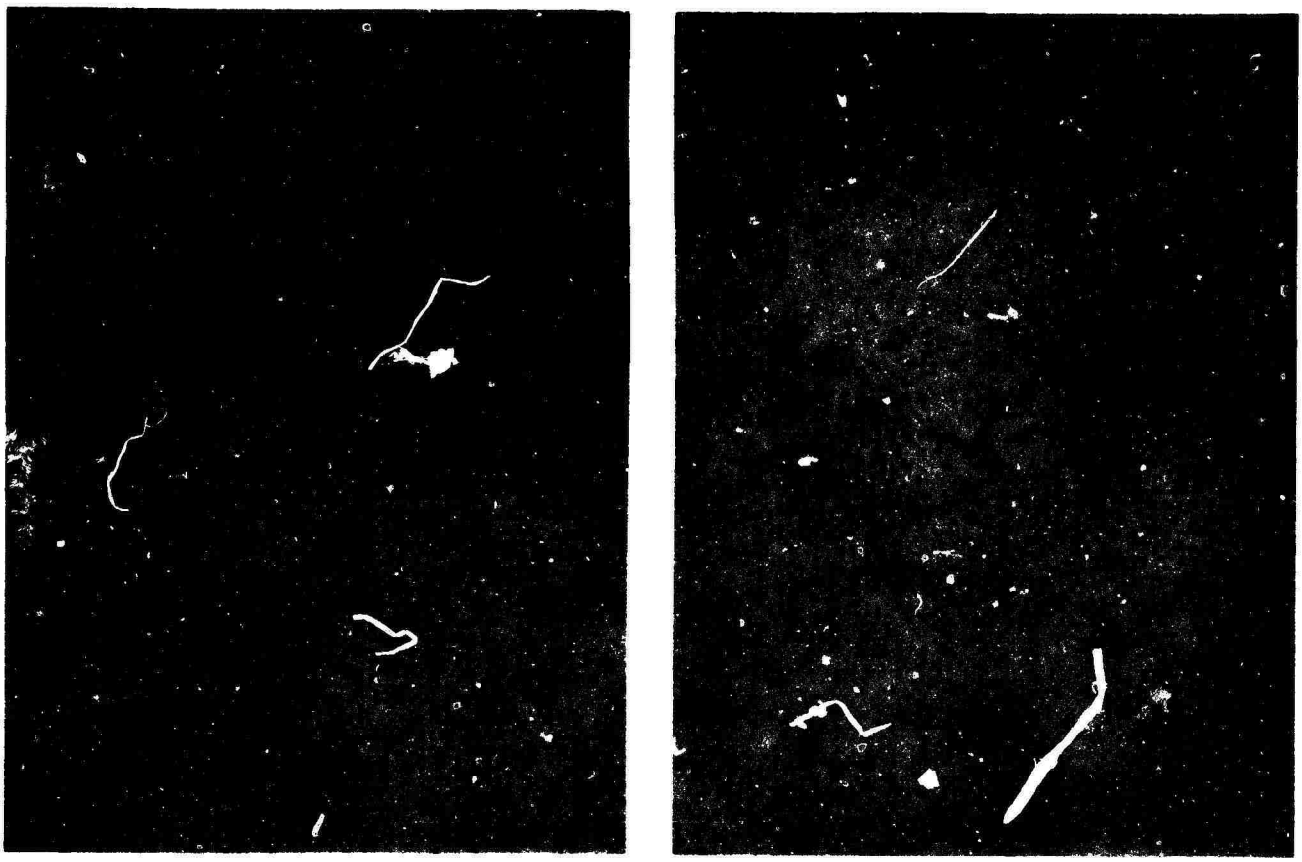

625X
+500 Volt sample

625X
500 Volt sample

Figure 14

Photomicrographs of Nichrome strips
exposed to 2 hours in flame

Ni

S

Sem

Nickel Overcoat

Cr

Plate 1: Scanning Electron Micrograph and X-ray Images
(Nichrome held at 500 Volts)
Mag. 500X

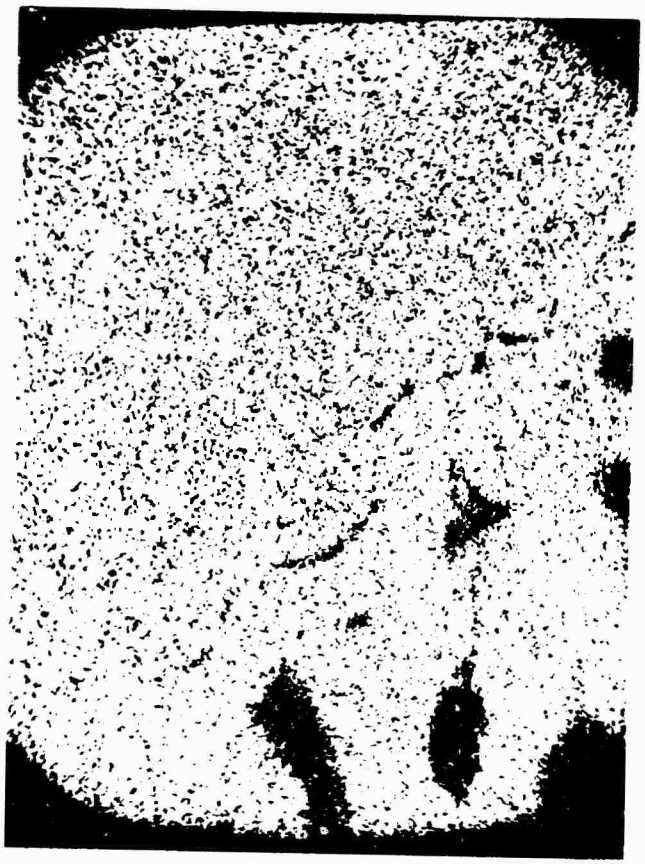

Ni

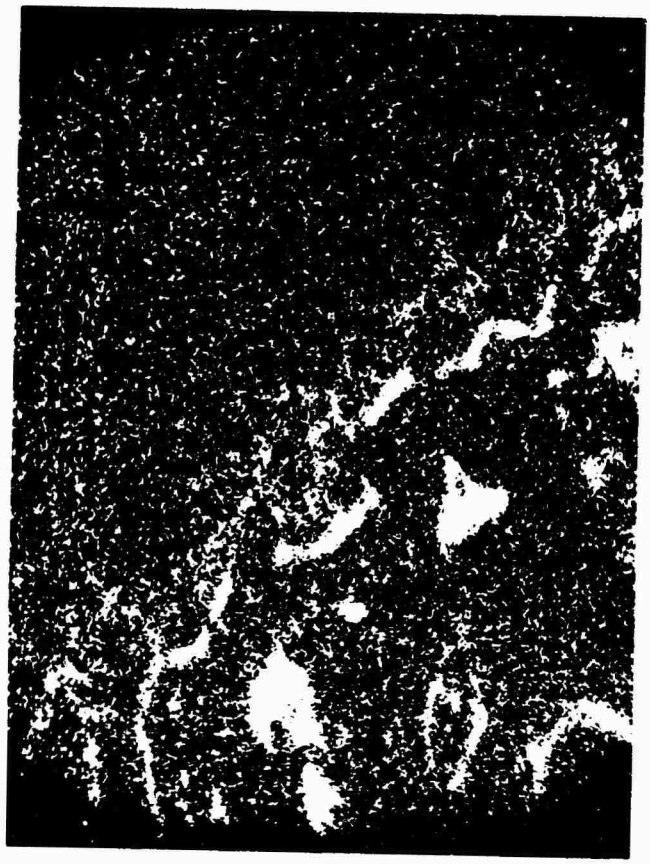

S

Sem

Cr

Plate 2: Scanning Electron Micrograph and X-ray Images
(Nichrome held at 500 Volts)
Mag. 500X

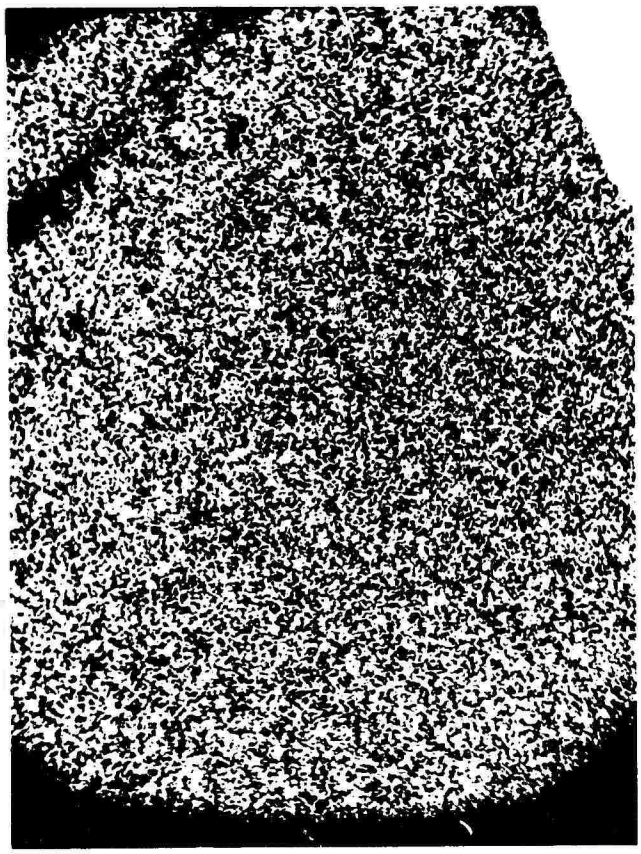

Ni

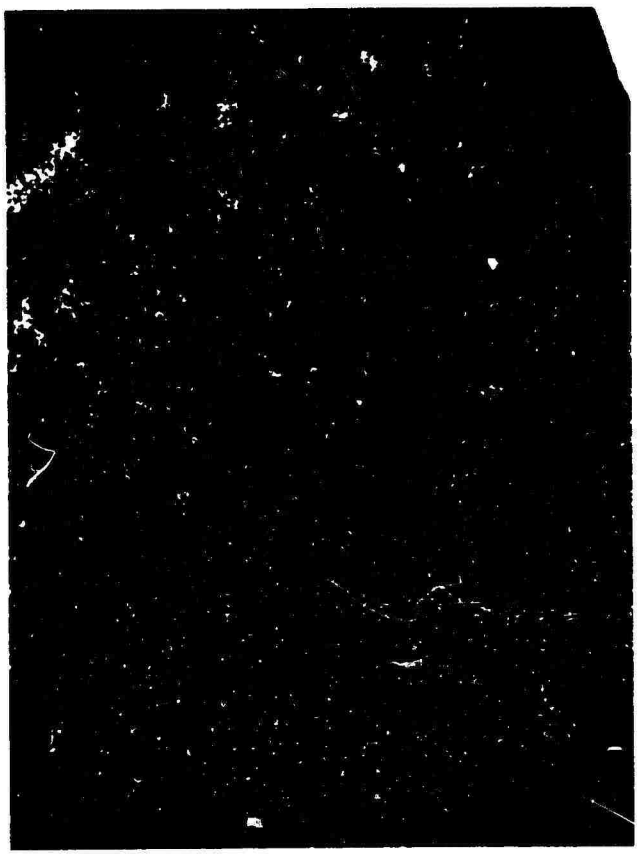

S

Sem

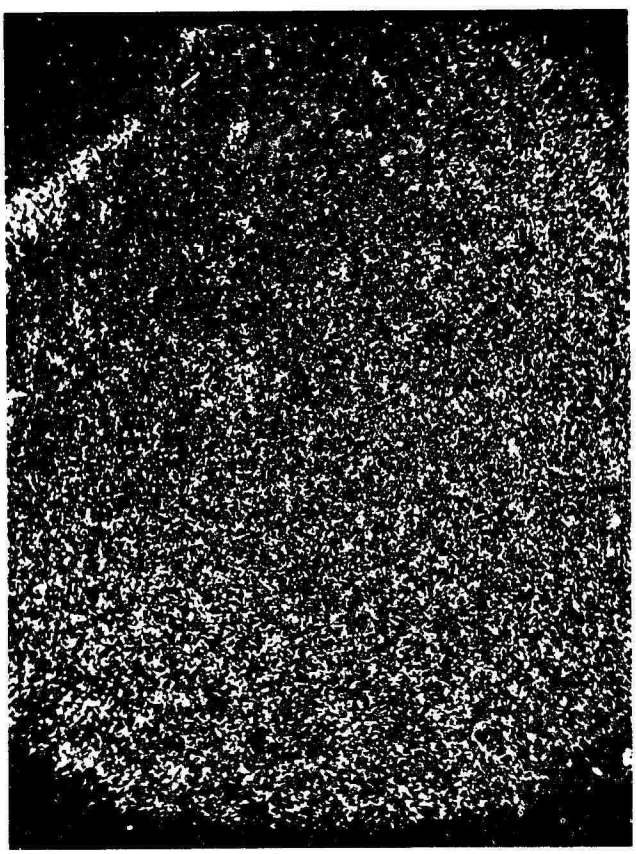

Cr

Plate 3: Scanning Electron Micrograph and X-ray Images
(Nichrome held at + 500 Volts)
Mag. 1000X

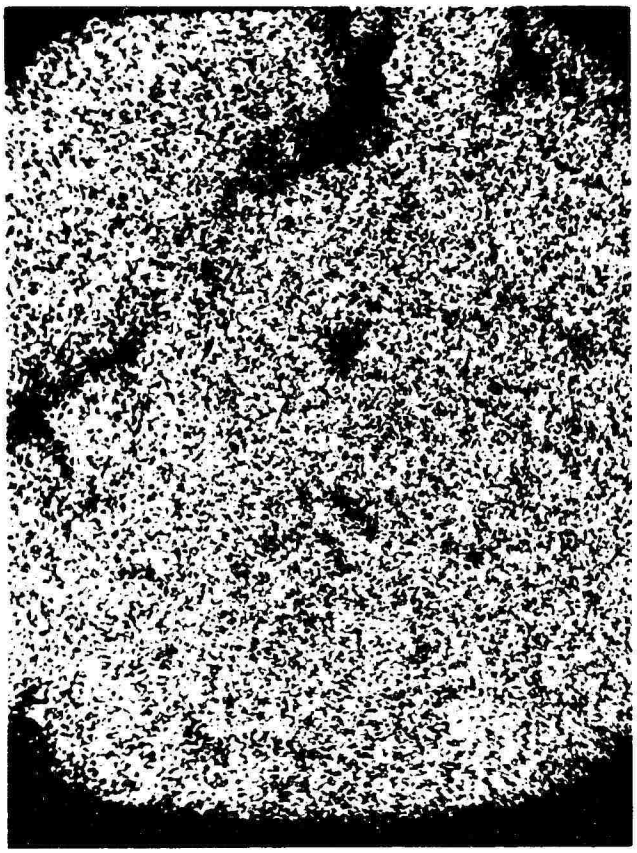

Ni

S

Sem

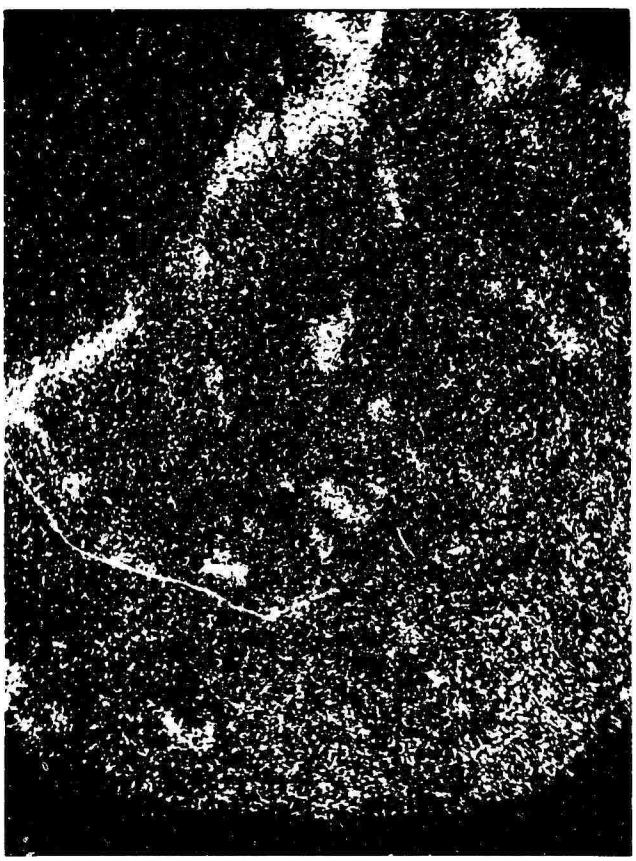

Cr

Plate 4: Scanning Electron Micrograph and X-ray Images
(Nichrome held at + 500 Volts)
Mag. 2000X

Based upon these observations, one can conclude that for the cathodic sample, the principal mechanism for surface attack is by oxidation. For the anodic sample, the degree of oxidation has been substantially reduced. Both samples exhibit the presence of sulfide precipitates.

2. Nickel, Hastelloy X and Co-Cr-Al-Y

Flame tests were done on nickel, Hastelloy X, and on Co-Cr-Al-Y alloy to further explore the effect of an applied field on hot corrosion in a salt seeded flame. Test conditions are summarized in Table 8. The samples were analyzed metallographically, with the following results.

Pure nickel rod was obtained and cylindrical samples were cut from this to be used in the flame test. The samples were suspended with a platinum wire by mechanically fixing the wire through a small hole drilled in the sample. The duration of the tests was determined by visual examination of the effect of the flame on the sample. After five hours of tests, significant surface alterations suggested that corrosion of a sample had been initiated. Metallographic examination showed corrosion to proceed primarily along grain boundaries, but no significant differences were observed among anodic, cathodic and unpolarized samples. Strip Hastelloy X samples were obtained and were exposed to the standard 2-hour exposure. No field effects were discernable optically by metallographic examination of samples held at +500, -500, and 0 volts. Strip Co-Cr-Al-Y samples were prepared from a single plate of material. Seven of these samples were used in the seven sample tester array to give a uniform exposure under different current conditions. Macrophotographs shown in Figure 15 show a highly variable degree of corrosion, apparently most extensive in the floating electrode and somewhat reduced at both positive and negative currents. The data are insufficient to establish a definitive relationship between corrosion rate and current density. They do suggest that Co-Cr-Al-Y, or aluminum oxide forming alloys generally might be good candidates for further study.

TABLE 8

FLAME TESTS

CYLINDRICAL NICKEL TESTS

Volts	Microamps	Exposure, 5 hours
-500	32	
0	0	
+500	850	

STRIP HASTELLOY X

Volts	Microamps	Exposure, 2 hours
-500	50	
0	0	
+500	7500	

STRIP Co-Cr-Al-Y

Volts	Microamps	Exposure, 3 hours
+500	400	
+400	50	
+ 80	10	
-500	20	
-300	12	
- 75	3	
0	0	

Figure 15
Co - Cr - Al - Y
from 7 Ball Array
Mag 9.9X

IV. DISCUSSION

The rate of corrosion of Nichrome strip samples in sodium sulfate melts open to air can generally be reduced by the application of an anodic potential. The relationship between anodic current density and degree of corrosion, however, varies with alloy structure, composition, and geometry. Application of cathodic potentials generally accelerates the rate of corrosion of Nichrome strip.

The mechanism of hot corrosion of nickel-chromium alloys has never been firmly established. Although there seems to be general agreement that sodium sulfate plays a critical role, there is considerable controversy about the precise nature of that critical role. The following mechanism, which has appeared in the literature, provides some insight into the possible effects of applied anodic or cathodic potentials. Mechanistic steps that have been proposed include:

1. Initially a protective scale of Cr_2O_3(s) and/or spinel is formed at the alloy surface.

2. The integrity of the protective scale is impaired, possibly by a reaction between Na_2SO_4 and Cr_2O_3 to form Na_2CrO_4:[4]

$$2Na_2SO_4 + Cr_2O_3 + \frac{1}{2}O_2 \longrightarrow 2Na_2CrO_4 + 2SO_2 \qquad (3)$$

possibly by dissolution of Cr_2O_3, although the measured solubility of Cr_2O_3 in Na_2SO_4 at 950°C is only 0.007%.

3. Once a path has opened through which Na_2SO_4 may penetrate to the alloy matrix, reduction can occur, which in the case of nickel based alloys might proceed by a reaction of the form:

$$Na_2SO_4 + \frac{9}{2}\,Ni \longrightarrow Na_2O + 3NiO + \frac{1}{2}\,Ni_3S_2 \qquad (4)$$

The Ni and Ni_3S_2 are present as a eutectic liquid.

4. Chromium from the alloy tends to displace nickel in the eutectic liquid with the formation of chromium sulfide:

$$\frac{x}{2}\,Ni_3S_2(l) + Cr(soln) \longrightarrow CrS_x + \frac{3x}{2}\,Ni(soln) \qquad (5)$$

5. The chromium depleted matrix is less oxidation resistant than the original alloy and is rapidly attacked by oxygen.

6. Penetration of Na_2SO_4(l), sulfidation, and oxidation result in a porous structure through which incompletely reacted Na_2SO_4(l) can penetrate still further, and the whole process propagates deeply into the base alloy.

If chromate formation, as in reaction (3), is indeed responsible for destroying the integrity of a normally protective Cr_2O_3 scale, then application of an anodic potential might reverse the reaction as follows:

$$\text{Anode:}\quad 2CrO_4^{=} \longrightarrow Cr_2O_3 + \frac{5}{2}\,O_2 + 4e^{-} \qquad (6)$$

By the same token, the rate of $CrO_4^{=}$ formation, and presumably loss of Cr_2O_3 as a protective scale, would be enhanced by reversal of equation (6) at the cathode. If reaction (4) contributes to accelerated oxidation by reaction of oxide ions ($O^{=}$) with nickel oxide formed to yield nickelate ions ($NiO_2^{=}$) which are soluble in the molten salt, then once again, the reaction could be suppressed at the anode and accelerated at the cathode. Similarly, sulfide ions, also believed to be active species in hot corrosion, could be stabilized in the vicinity of the cathode and could be converted to presumably less active S_2 in the vicinity of the anode. Interpretation is difficult, however, since the actual cathodic and anodic reactions in flames are unknown.

Observations of far more rapid corrosion of nichrome strip than of nichrome sphere samples in molten sodium sulfate point up the importance of structural factors in hot corrosion. Easy diffusion paths in the strip samples undoubtedly promote attack by sodium sulfate at edges and corners, leading to delamination and exfoliation as the corrosion reaction proceeds.

Possibilities for Modifying the Rate and Mechanism of Hot Corrosion in Flames by Application of Electrical Potentials

Mobility of Ionic Species in Flame and in Molten Salt

Throughout the experimental program on the effect of electric fields on hot corrosion in flames, a simple physical model of the corrosion process in a flame has been used. In this model, hot corrosion is assumed to be initiated by the formation of a molten salt layer on the metal surface and subsequent attack by chemical species is assumed to be similar to that found in molten salt systems. Two features of the experimental process which lead to this simplification are: (1) observations during flame tests indicating the formation of a thin film of molten salt on the metal; and (2) observation of maximum corrosion in the temperature range where the salt in the seeded flame is molten. Furthermore, the temperature of maximum corrosion in the flame is the same temperature at which corrosion in a pure molten salt experiment is observed.

Since numerous tests show marked effect of the application of an electrical field on corrosion in molten salt experiments it was felt that similar results could be obtained in the salt seeded flame. However, an important feature of the ionic mobility of the flame species may account for the somewhat dissimilar results. The flame conductivity is dominated by the high mobility of the electrons, which move at about 2600 cm/sec, while the heavier weight positive ionic species travel at only about 2 cm/sec. This phenomenon in flames is well known and accounts for the fact that high currents are observed when sample electrodes are

positive and able to attract the electronic species, while lower currents are observed with negative electrodes which must move the large nearly immobile positive charge carriers. This diode like effect is shown in Figures 16 and 17.

In molten salt bath tests both the negative and positive species are ions, which have equal mobility and share in the electrochemical reaction between electrodes. In the flame tests, positive ions and electrons are the only charged species, and the interaction between electrodes is by the electrons which traverse the flame. The absence of negative ions and the very different behavior of positive ions in the flame tests, may account for the absence of dramatic corrosion protection as seen in the molten salt bath tests.

Conditions for Observing Electric Field Effects in Hot Corrosion

If the parabolic growth mechanism were applicable to hot corrosion of high chromium content nickel based alloys, then, as shown in the Appendix, currents of at least 12 milliamps/cm^2 would have to be passed through the growing scale in order to change corrosion rates by as much as 20% in the 30 minute to 2 hour periods of our experiments. The highest current levels actually observed in the flame were of the order of 0.2 milliamps/cm^2, at least a factor of 60 too small.

In the flame test apparatus used for the studies to date, a maximum current density of 0.5 milliamps/cm^2 might be achievable at sample temperatures of 910 to 960°C. Calculations given in the Appendix show that at this current level, Cr_2O_3 would have to build up, on a chromia scale forming alloy following the Wagner mechanism, to a thickness of more than three centimeters before scale growth could be stopped by application of an electric field. This is greater than the diameter of the spherical samples (0.61 cm) used in many of our experiments.

It should be pointed out that electrical conductivity in salt seeded flames increases very markedly with temperature. Changes in the rate of scaling may therefore be more readily observable at temperatures above 1000°C, which is outside of the range of normal hot corrosion, but which is still of interest for advanced engines.

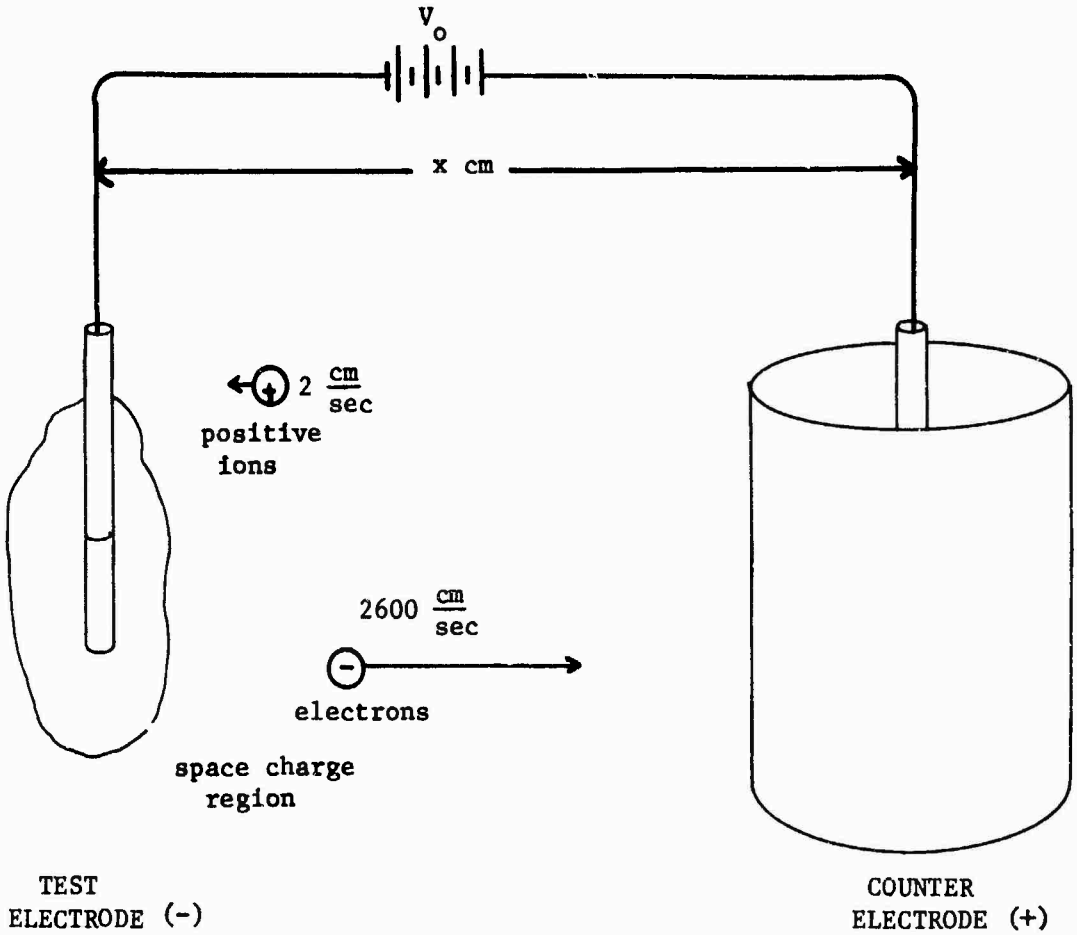

FIGURE 16

MOBILITY OF POSITIVE IONS AND ELECTRONS
IN FLAME UNDER AN APPLIED POTENTIAL
OF Vo/x per cm

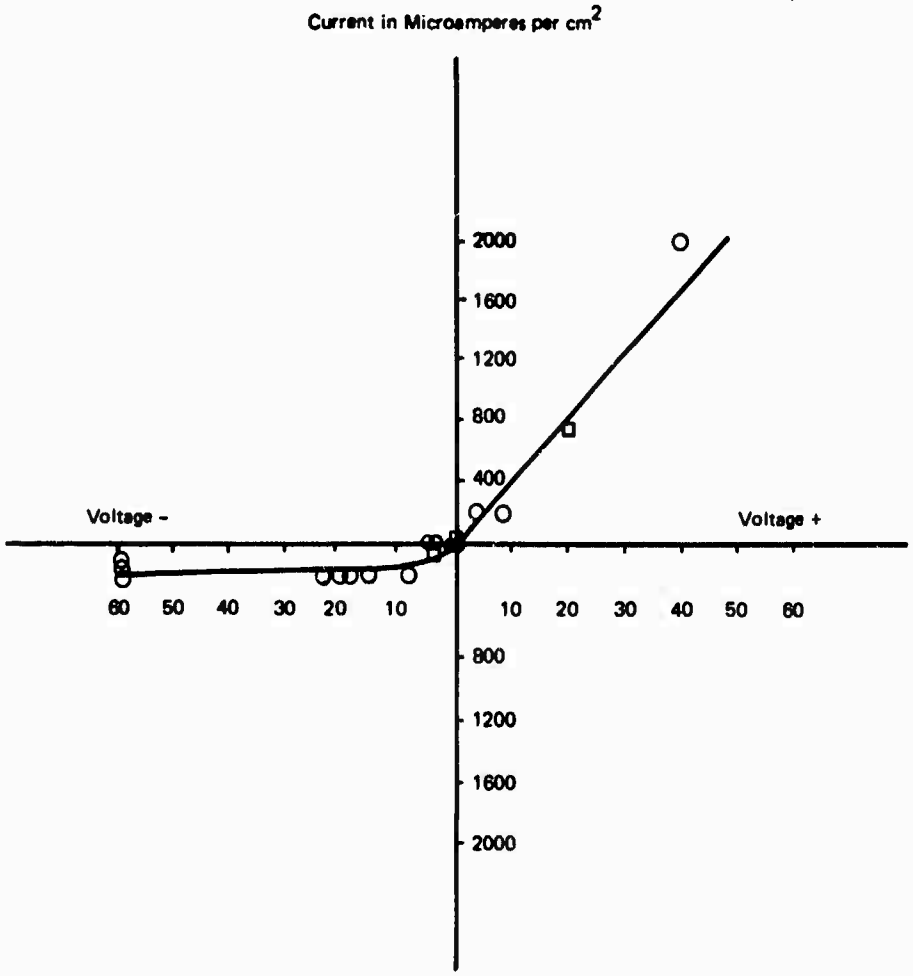

FIGURE 17 TYPICAL CURRENT/VOLTAGE CHARACTERISTIC IN SODIUM SULFATE SEEDED FLAMES

Applicability of Wagner Mechanism to Hot Corrosion

While the parabolic growth theory of scale formation provides a coherent explanation of the possible mechanism of affecting hot corrosion with an applied electric field some observations, discussed in the following paragraphs are not perfectly consistent.

Simply viewed, the electrical network looks like a series connection of resistances as shown below.

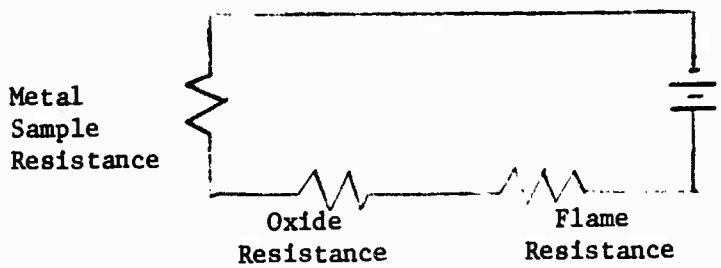

A series of tests was performed to determine the effects of flame resistivity. A platinum electrode was used in the system and the current was maintained for an hour. The voltage was observed to remain constant. Since platinum does not oxidize in the flame, the consistency of the test confirmed that the flame resistancy does not change, since the sample resistance and oxide resistance were also fixed.

With Inconel 600 spheres used as samples the voltage was seen to vary while the current was held fixed. In tests 73-25B through 73-34B (see Section III) the system resistivity was observed to fall by about 10%. The decline in resistivity of the system is shown in the following figure (Figure 18), in which the current is seen to rise as the voltage remains fixed. Also shown are data points taken prior to the test with a platinum electrode in the flame. The gradual increase in current with the platinum electrode is due to the warm up of the furnace. Once the platinum electrode reached equilibrium the test with the Inconel 600 sphere was initiated.

It is possible that as molten salt collected on the sample during the test, the effective resistance of the oxide decreased due to the high conductivity of the molten salt. The presence of a highly conductive medium could lower the overall resistance by several means; the molten salt might provide a path to the sample, effectively eliminating the resistance of the oxide as it grows in thickness with exposure to the salt seeded flame.

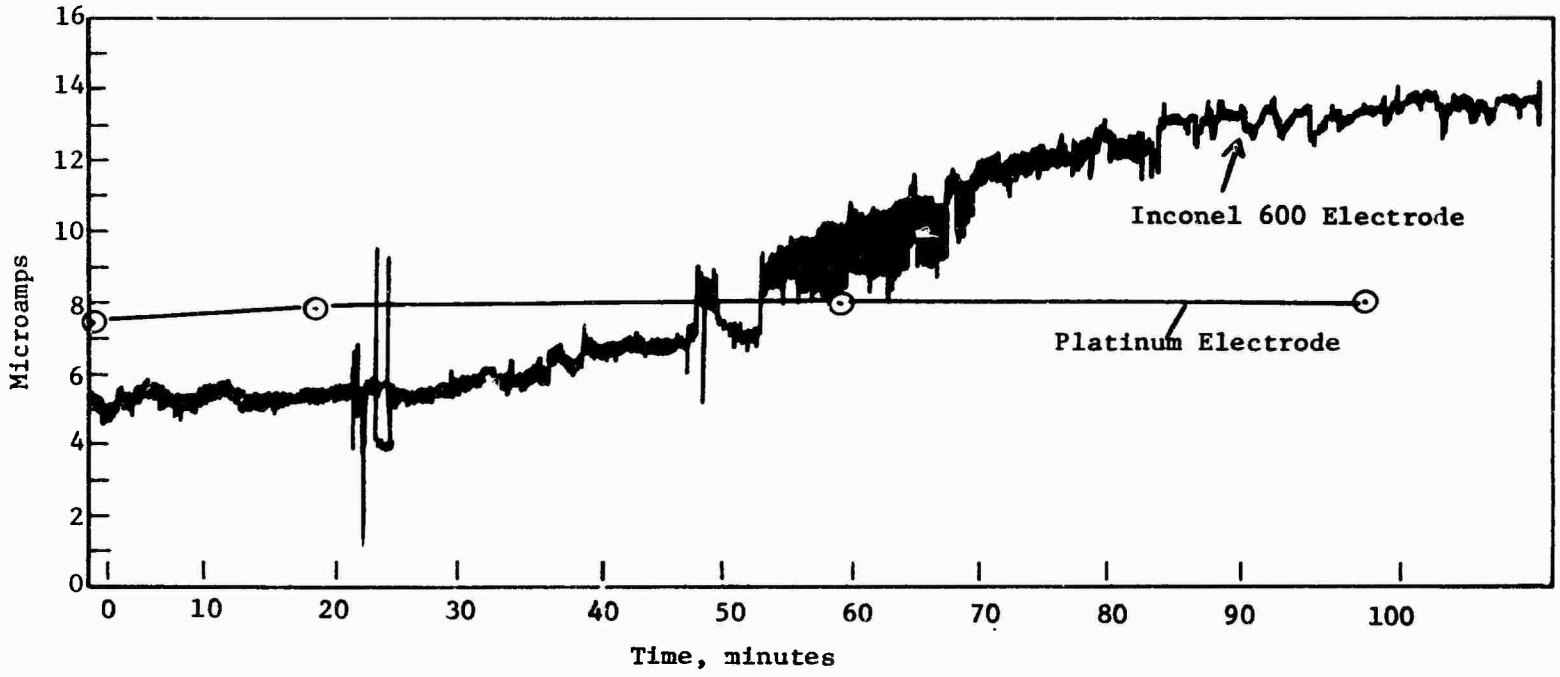

FIGURE 18

CHANGE IN CURRENT AT CONSTANT VOLTAGE FOR
INCONEL 600 and PLATINUM WORKING ELECTRODES

V. CONCLUSIONS AND RECOMMENDATIONS

Although the application of electric fields in flames at temperatures in the neighborhood of 900°C, where the flame conductivity is low, did not appear to alter the observed rate of corrosion of chromium oxide forming alloys significantly, nonetheless evidence was found for a modification of mechanism. Observations of enhanced oxidation, as opposed to sulfidation, at the cathode and decreased oxidation at the anode are consistent with the relative oxide activities at each electrode.

The basic electrochemistry of salt seeded flame systems, and more particularly the fundamental chemistry of electrode reactions in flames, is virtually unexplored. Although the same techniques that have been used to study electrode reactions in aqueous and molten salt systems should be adaptable to flames, the seeded flame is a unique electrolyte in two respects:

(1) The conducting species are highly mobile electrons and relatively slow moving positive ions, rather than positive and negative ions of about equal mobility.

(2) The current levels achievable for a given voltage, even in a seeded flame, are orders of magnitude less than those in aqueous or molten salt electrolytes.

Nonetheless, seeded flames can in principal be studied by such electroanalytical methods as voltammetry, chronopotentionometry, and polarization curve determinations. One of the first and most important problems to be solved in carrying out a meaningful electrochemical investigation is the development of stable, reproducible and nonpolarizable reference electrode systems. Data on the fundamental kinetics and mechanisms of electrode/flame interactions could provide a firm basis for further exploration of practical electrochemical control methods for marine turbine corrosion.

References

1. P.J. Jorgensen, J. Electrochem. Soc., 110, 461 (1963).

2. P.J. Jorgensen, J. Chem. Phys., 37, 874 (1962).

3. C. Wagner, Considerations on the Effect of an External Electrical Field Applied to an Oxide Layer Growing in a Metal in Oxygen, memorandum from the personal files of Paul Jorgensen.

4. F.A. Kroger, The Chemistry of Imperfect Crystals, North Holland Publishing Co., Amsterdam (1964), 852.

5. F.A. Kroger, Proceedings of British Ceramic Society, 1, 167 (1964).

6. P. Kofstad, High Temperature Oxidation of Metals, John Wiley and Sons, Inc., New York (1966).

7. H.H. Uhlig, Acta Met., 4, 541 (1965).

8. S.A. Hoenig and J.R. Lane, Surface Science, 11, 163 (1968).

9. N.S. Bornstein, M.A. DeCrescente, and H.A. Roth, Annual Report for Office of Naval Research, Contract N00014-70-C-0234 (1972).

10. J.A. Goebel and F.S. Pettit, Met. Trans., 1, 1943 (1970).

11. Berkowitz, J., Arthur D. Little, Inc., Effect of Applied Electric Fields on the Mechanisms of Oxidation of Metals and Alloys, Department of the Navy, Contract No. N00019-72-C-0217, Dec. 1971 to Dec. 1972.

12. E.L. Simons, G.V. Browning, and H.A. Liebhafsky, Corrosion, 11, 17 (1955).

13. Powling, J.A. Fuel London 28 25 1949
Egerton, Sir Alfred SK Proc. R. Soc. A21[illegible] 45, 1952.

14. Worthberg, G. 10th Ion Symp. Combustion, p. 651

15. International Critical Table VI, page 145.

16. T. Wlodek, Trans. of the AIME 230, 177 (1964).

APPENDIX

Conditions for Measurable Electric Field Effects on Scale Growth

For parabolic scale growth discussed earlier, the passage of a current I_{ext} alters the scale growth rate as follows*:

$$\frac{dn}{dt} = \left(\frac{dn}{dt}\right)_o - \frac{I_{ext}}{erb} (t_M + t_X)$$

where $\left(\frac{dn}{dt}\right)_o$ is growth rate in the absence of a current.

The integral of the growth rate equation from time 0 to time t is:

$$n(t) = n_o(t) - \frac{I_{ext}}{erb} (t_M + t_X)\, t$$

where the thickness of the initial scale at the start of the test is zero.

In order to effect a demonstrable change in the growth of scale n (t) with and without an applied current, the change of scale thickness must be large compared to the accuracy of the measurement technique. Therefore

$$\frac{n_o(t) - n(t)}{n_o(t)} >> \text{experimental accuracy}$$

It is believed that such an observation could be made if

$$\frac{n_o(t) - n(t)}{n_o(t)} > .20; \text{ if, i.e.,}$$

$$\frac{n_o(t) - n(t)}{n_o(t)} = \frac{\frac{I_{ext}}{erb} (t_M + t_X)\, t}{n_o(t)} > .20$$

*Symbols are defined on page A5.

Therefore the criterion for demonstrating the slowing of scale growth requires that

$$I_{ext} > .20 \left[\frac{n_o(t)}{t} \quad \frac{erb}{t_M + t_X} \right]$$

Since $(t_X + t_M)$ is a maximum of 1, the minimum current necessary to given demonstrable reduction in scale growth is

$$I_{ext} > .20 \left[\frac{n_o(t)}{t} \quad erb \right] \qquad (1)$$

where

e = 1.6×10^{-19} coulombs

r = valence of negative ions

b = number of negative ions in scale molecule

$\frac{n_o(t)}{t}$ = scale growth in molecules/cm^2/sec at time t

For a spherical sample exposed to a salt seeded flame:

$$\frac{n_o(t)}{t} = \frac{\Delta V}{t} \frac{\rho}{M} \times 6 \times 10^{23}$$

where

ρ = scale density in grams/cm^3

M = scale molecular weight

6×10^{23} = number of molecules per mole (Avogadro's Number)

$\frac{\Delta V}{t}$ = volume of scale per time t exposure to flame

Since the definition of % corrosion measured through the program is

$$\frac{\Delta V}{V} = \% \text{ corrosion}$$

where V is the initial volume of the sphere then the average volume growth rate of scale is $\frac{\text{(X corrosion)}}{\text{exposure time}}$

and hence;

$$\frac{n_o(t)}{t} = \frac{\Delta V}{t} \frac{\rho}{M} \frac{\% \text{ corrosion}}{A}$$

where

A = is the average surface area over which corrosion takes place which is approximately $4\pi r_s^2$ where

r_s = is the sample radius

t = exposure duration

therefore

$$\frac{n_o(t)}{t} = \frac{1/3\ r_s\ (\%\ \text{corrosion})}{t} \quad \frac{\rho}{M} \times 6 \times 10^{23} \qquad (3)$$

Combining equation (3) and (1)

$$\left(I_{ext}\right)_{min} > \left(3.2 \times 10^4\ rbr_s \quad \frac{(\%\ \text{corrosion})}{\Delta t} \quad \frac{\rho}{M}\right)$$

The scale formed in hot corrosion is a complex one, possibly including the following constituents, listed with calculated minimum currents for influencing corrosion rates by 20%.

Substances

	P	M	r	b	$\left(I_{ext}\right)^*_{min}$
Ni_3S_4	4.7	304	3	4	65.6 milliamps/cm^2
Cr_2S_3	3.77	200	2	3	12.0 milliamps/cm^2
Cr_2O_3	5.21	152	2	3	72.0 milliamps/cm^2

This compares with the highest current levels obtained in the flame of about 0.2 milliamps/cm^2 a factor of 60 too small in current flux.

For the spherical balls tests a level of current 60 times as great as those which could be obtained in the salt seeded flame would be necessary to retard the growth of scale, measured to be about 10% of the sphere in 30 minutes.

** Based on measure % corrosion = 10% after 1/2 hour under zero current for a 1/8" radius sample of Inconel 600 sphere.

With the current levels developed in the flame tests to date, a maximum of .5 milliamps per cm^2 for a spherical sample could be expected at sample temperatures of 910°C to 960°C. The thickness of the scale necessary to stop the scale growth rate, when an applied external current of .5 milliamps per cm^2 is maintained is governed by:

$$\Delta X\Big|_{Stop} = \frac{E\sigma}{I_{ext}}$$

where E is determined by the free-energy change of the scale-forming reaction ($\Delta G = -nFE$) and σ is the scale conductivity in $ohm^{-1}\ cm^{-1}$. For Cr_2O_3, E ≈ 1.35 volts and hence if Cr_2O_3 were the scale forming oxide, and the Wagner mechanism were applicable, the oxide would build up to a thickness ΔX given by:

$$\Delta X(cm) = \frac{1.35\ \sigma}{.5 \times 10^{-3}}$$

$$= 2.7 \times 10^{3}\ \sigma$$

before scale growth could be stopped by application of an electric field.

If the scale is unaltered by the molten salt collecting on it, then the scale resistivity would be expected to be that of the scale products. The scale products are nickel and chromium oxides. The conductivity[15] of these oxides at 700°C are:

Oxide	σ	
NiO_x	10^{-3}	$(ohm\text{-}cm)^{-1}$
Cr_2O_3	1.2×10^{-3}	$(ohm\text{-}cm)^{-1}$

and the resulting scale thickness for the retardation of these oxide growths for an applied current of .5 $milliamps/cm^2$ would be:

Oxide	ΔX (cm)
NiO_x	2.7
Cr_2O_3	3.24

Whether or not the molten salt affects the conductivity of oxide layer, the thickness required to develop sufficient halting voltage at .5 $milliamp/cm^2$ applied current is greater than the diameter of the spherical samples (.61 cm dia).

List of Symbols

a,	number of metal atoms in the oxide molecule M_aO_b
b,	number of oxygen atoms in the oxide molecule M_aO_b
$\frac{dn}{dt}$,	oxide growth rate (molecules/cm^2-sec) in the presence of an electric field
$\left(\frac{dn}{dt}\right)_o$,	normal oxide growth rate in the absence of an external electric field
I_{ext},	current flow (amperes) through the oxide scale
e,	charge on the electron, coulombs
r,	valence of the negative ions ($r = 2$ for $O^=$ ions)
t_M,	transference number of metal ions in the oxide scale
t_X,	transference number of oxide ions in the oxide scale
E_{ext},	ok potential across the oxide scale
$\Delta\chi$,	thickness of the oxide scale
t,	time (seconds)
σ,	electrical conductivity of the oxide scale
E,	voltage charge associated with the free energy (ΔG) of the corrosion reaction